

Transcriptional regulation by NR5A2 links differentiation and inflammation in the pancreas

Isidoro Cobo¹, Paola Martinelli^{1†*}, Marta Flández^{1†*}, Latifa Bakiri², Mingfeng Zhang³, Enrique Carrillo-de-Santa-Pau¹, Jinping Jia³, Víctor J. Sánchez-Arévalo Lobo^{1†}, Diego Megías⁴, Irene Felipe¹, Natalia del Pozo^{1,5}, Irene Millán^{1,5}, Liv Thommesen⁶, Torunn Bruland^{7,8}, Sara H. Olson⁹, Jill Smith¹⁰, Kristina Schoonjans¹¹, William R. Bamlet¹², Gloria M. Petersen¹², Núria Malats^{13,14}, Laufey T. Amundadottir³, Erwin F. Wagner² & Francisco X. Real^{1,5,15}

Chronic inflammation increases the risk of developing one of several types of cancer. Inflammatory responses are currently thought to be controlled by mechanisms that rely on transcriptional networks that are distinct from those involved in cell differentiation^{1–3}. The orphan nuclear receptor NR5A2 participates in a wide variety of processes, including cholesterol and glucose metabolism in the liver, resolution of endoplasmic reticulum stress, intestinal glucocorticoid production, pancreatic development and acinar differentiation^{4–8}. In genome-wide association studies^{9,10}, single nucleotide polymorphisms in the vicinity of NR5A2 have previously been associated with the risk of pancreatic adenocarcinoma. In mice, Nr5a2 heterozygosity sensitizes the pancreas to damage, impairs regeneration and cooperates with mutant Kras in tumour progression¹¹. Here, using a global transcriptomic analysis, we describe an epithelial-cell-autonomous basal pre-inflammatory state in the pancreas of Nr5a2^{+/-} mice that is reminiscent of the early stages of pancreatitis-induced inflammation and is conserved in histologically normal human pancreases with reduced expression of NR5A2 mRNA. In Nr5a2^{+/-} mice, NR5A2 undergoes a marked transcriptional switch, relocating from differentiation-specific to inflammatory genes and thereby promoting gene transcription that is dependent on the AP-1 transcription factor. Pancreatic deletion of Jun rescues the pre-inflammatory phenotype, as well as binding of NR5A2 to inflammatory gene promoters and the defective regenerative response to damage. These findings support the notion that, in the pancreas, the transcriptional networks involved in differentiation-specific functions also suppress inflammatory programmes. Under conditions of genetic or environmental constraint, these networks can be subverted to foster inflammation.

The relationship between germline Nr5a2 haploinsufficiency, mutant Kras and inflammation in promoting pancreatic adenocarcinoma (PDAC) suggests functional interactions that may be relevant to human disease¹¹. In two independent groups of patients with PDAC, tumours with lower levels of NR5A2 expression were significantly enriched in patients with a history of chronic pancreatitis ($P = 0.001$) (Supplementary Table 1). The rs3790844 risk-increasing allele (T), which is associated with increased susceptibility to pancreatic cancer⁹, is also associated with reduced NR5A2 protein levels ($P = 0.028$,

$\beta = -0.57$) (Extended Data Fig. 1). This suggests that NR5A2 expression may underlie susceptibility to PDAC.

We used Nr5a2^{+/-} mice to identify the mechanisms that favour impaired regeneration in the pancreas and PDAC. The pancreas of an adult Nr5a2^{+/-} mouse is histologically normal, as are its expression of pancreatic transcription factors and digestive enzymes (Extended Data Fig. 2a, b). RNA sequencing (RNA-seq) showed that 926 and 100 genes were significantly upregulated or downregulated, respectively, in pancreases from 8–10-week-old Nr5a2^{+/-} mice, when compared to wild-type mice. Gene set enrichment analysis (GSEA) revealed that 21 out of 23 gene sets that were over-represented in Nr5a2^{+/-} mice, and 68% of upregulated genes, belong to inflammatory pathways (Fig. 1a, b and Supplementary Tables 2, 3). Among these genes are those coding for chemokines (*Ccl5* and *Ccl7*), complement components (*C1qb* and *C3*) and metalloproteases. Results were confirmed by quantitative PCR (qPCR) with reverse transcription (qRT-PCR) (Fig. 1c). Corresponding changes in H3K27ac or H3K27me3 at the promoters of differentially regulated genes were also observed (data not shown). mRNA and protein analyses using fresh tissue, isolated acini and immunohistochemistry confirmed upregulation of inflammatory mediators in acinar cells (Fig. 1c–e and Extended Data Figs 2c, 3a). Quantification of Cd45⁺ cells and immune-cell populations in wild-type and Nr5a2^{+/-} pancreases did not reveal significant differences between the two, and a role for a ductal cell contribution to inflammatory gene expression was excluded (Fig. 1f and Extended Data Figs 2d–f, 3). Pancreas-selective inactivation of one Nr5a2 allele, and biallelic Nr5a2 inactivation in myeloid cells, showed that the defect is specific to pancreatic epithelial cells (Extended Data Fig. 4), which indicates that Nr5a2 haploinsufficiency generates an epithelial-cell-autonomous basal pre-inflammatory state.

To assess whether similar transcriptomic changes occur in humans, we compared histologically normal pancreases ($n = 95$)¹² with high versus low NR5A2 expression (top versus bottom quartile) ($n = 24$ per group). Seventy-eight per cent of genes for which expression was upregulated in Nr5a2^{+/-} pancreases ($n = 718$) were also differentially expressed in human samples ($P < 0.05$). Of these differentially upregulated genes, 92% were significantly upregulated. By contrast, 44% of downregulated genes ($n = 64$) were differentially represented ($P < 0.05$) and only 50% of them were downregulated (Fig. 1g). Overall, genes that were upregulated in Nr5a2^{+/-} mice were also upregulated

¹Epithelial Carcinogenesis Group, Spanish National Cancer Research Centre-CNIO, Madrid, Spain. ²Genes, Development, and Disease Group, Spanish National Cancer Research Centre-CNIO, Madrid, Spain. ³Laboratory of Translational Genomics, Division of Cancer Epidemiology and Genetics, National Cancer Institute, National Institutes of Health, Bethesda, Maryland 20892, USA. ⁴Confocal Microscopy Unit, Spanish National Cancer Research Centre-CNIO, Madrid, Spain. ⁵Epithelial Carcinogenesis Group, Spanish National Cancer Research Centre-CNIO, CIBERONC, Madrid, Spain. ⁶Department of Biomedical Science, Norwegian University of Science and Technology (NTNU), Trondheim, Norway. ⁷Clinic of Medicine, St. Olav's University Hospital, Trondheim, Norway. ⁸Department of Clinical and Molecular Medicine, Norwegian University of Science and Technology (NTNU), Trondheim, Norway. ⁹Department of Epidemiology and Biostatistics, Memorial Sloan Kettering Cancer Center, New York, New York 10065, USA. ¹⁰Departments of Gastroenterology and Hepatology, Georgetown University, Washington, DC 20007, USA. ¹¹Ecole Polytechnique Fédérale de Lausanne, Lausanne, Switzerland. ¹²Division of Epidemiology, Department of Health Sciences Research, Mayo Clinic, Rochester, Minnesota 55905, USA. ¹³Genetic and Molecular Epidemiology Group, Spanish National Cancer Research Centre-CNIO, Madrid, Spain. ¹⁴Genetic and Molecular Epidemiology Group, Spanish National Cancer Research Centre-CNIO, CIBERONC, Madrid, Spain. ¹⁵Departament de Ciències Experimentals i de la Salut, Universitat Pompeu Fabra, Barcelona, Spain. †Present addresses: Medical University Vienna, Department of Medicine I, Institute for Cancer Research, Vienna, Austria (P.M.); Tissue Regeneration Laboratory, Spanish National Cardiovascular Research Centre-CNIC, Madrid, Spain (M.F.); Department of Biotechnology, Facultad de Ciencias Biosanitarias, Universidad Francisco de Vitoria, Pozuelo de Alarcón, Spain (V.J.S.-A.L.).

*These authors contributed equally to this work.

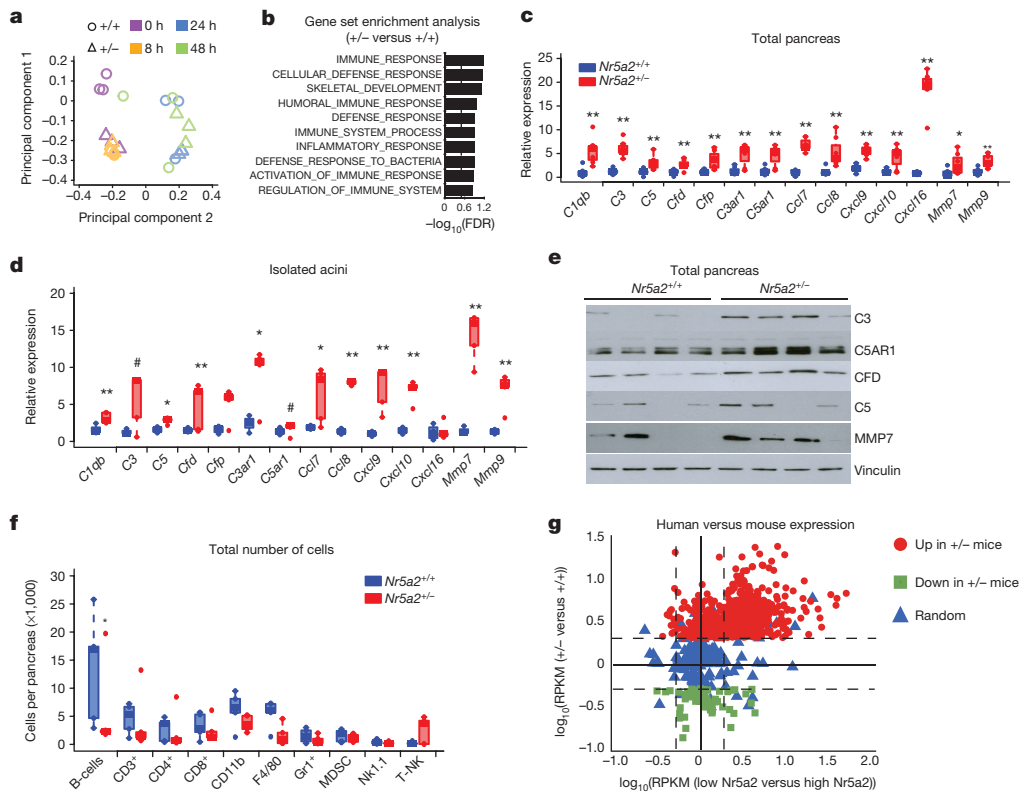


Figure 1 | Reduced NR5A2 expression is associated with pre-inflammation in normal pancreas of mice and humans. **a**, Principal component analysis of the transcriptome of wild-type (+/+) and $Nr5a2^{+/-}$ (+/-) mice in basal conditions and during caerulein-induced pancreatitis (seven injections, given once an hour) ($n = 3$ per group). **b**, GSEA of genes that are differentially expressed in $Nr5a2^{+/-}$ ($n = 3$) and wild-type mice ($n = 3$). **c**, qRT-PCR showing upregulation of inflammatory genes in $Nr5a2^{+/-}$ pancreases relative to wild type ($n = 7$ per group). **d**, qRT-PCR showing upregulation of inflammatory genes in primary $Nr5a2^{+/-}$ acinar

cells relative to wild type ($n = 4$ per group). **e**, Western blots showing upregulation of inflammatory proteins in $Nr5a2^{+/-}$ pancreases ($n \geq 4$ per group). **f**, Fluorescence-activated cell-sorting analysis of inflammatory cells in wild-type and $Nr5a2^{+/-}$ pancreases ($n = 4$ per group). **g**, Scatter plot showing the relationship between expression of upregulated, downregulated or a random set of genes in $Nr5a2^{+/-}$ versus control $Nr5a2^{+/+}$ mice (y axis) and in histologically normal human pancreatic samples (x axis, low versus top high quartiles of NR5A2 mRNA expression). In **c**, **d** and **f**, one-sided Mann-Whitney U test; * $P < 0.05$, ** $P < 0.01$.

in NR5A2^{low} versus NR5A2^{high} human pancreases, when compared with a random list of 173 genes ($P = 1 \times 10^{-31}$). By contrast, downregulated genes did not follow a concordant pattern in mouse and human pancreases ($P = 0.58$). The conservation of findings across species provides a framework for understanding the relationship between the NR5A2 genotype, NR5A2 mRNA expression and PDAC in mice.

Analysis of public ChIP-seq (chromatin immunoprecipitation followed by sequencing) datasets⁶ pertaining to pancreatic NR5A2 showed that the promoters of 89% of the genes that had upregulated expression in $Nr5a2^{+/-}$ mice contain putative NR5A2 binding sites, but only 7% actually exhibit NR5A2 binding within 2.5 Kb of the transcriptional start site. This suggests the participation of an indirect mechanism (Fig. 2a). Promoter scanning analysis of upregulated genes showed significant enrichment of AP-1 and NF- κ B binding motifs, among others. A similar enrichment was found when computing the list of upregulated genes with GSEA using the MSigDB C3 transcription factor target gene-set collection (<http://software.broadinstitute.org/gsea/msigdb/collections.jsp>). *Jun* (also known as *c-Jun*), *Junb*, *Jund* and *Fos* (also known as *c-Fos*) mRNA and their corresponding proteins were significantly upregulated in $Nr5a2^{+/-}$ pancreases (Fig. 2b, c). We confirmed that these changes occurred in epithelial cells using freshly isolated acini and immunohistochemistry (Extended Data Fig. 3g). Phospho-JUN (p-JUN) and phospho-JNK (p-JNK) were also upregulated in $Nr5a2^{+/-}$ pancreases and isolated acini (Fig. 2d and Extended Data Fig. 3h). ChIP followed by qPCR (ChIP-qPCR) showed significantly increased binding of NR5A2 to the promoters of *Fos* and *Fos1* (also known as *Fra1*)—but not to those of *Jun*, *Junb* and *Jund*—in $Nr5a2^{+/-}$ pancreases compared to wild-type mouse pancreases (Fig. 2e).

NR5A2 expression in human embryonic kidney (HEK293) cells led to a dose-dependent decrease of *JUN* mRNA (Fig. 2f), indicating that changes in NR5A2 levels can modulate *JUN* expression. ChIP-qPCR showed increased binding of JUN, JUNB, JUND and FOS to the promoter of upregulated inflammatory genes in $Nr5a2^{+/-}$ pancreases (Fig. 2g).

The basal pre-inflammatory transcriptome of $Nr5a2^{+/-}$ mice suggests a subclinical pancreatitis-like state. We compared the transcriptomes of wild-type and $Nr5a2^{+/-}$ pancreases 8, 24 and 48 h after induction of mild acute pancreatitis (with 7 doses of caerulein), using RNA-seq. Principal component analysis highlighted the divergence of the basal transcriptomes of wild-type and $Nr5a2^{+/-}$ pancreases; these differences were completely but transiently eroded 8 h after pancreatitis induction. The basal transcriptome of $Nr5a2^{+/-}$ pancreases was similar to that of wild-type mouse pancreases at 8 h (Fig. 1a). The differences between the set of genes upregulated in $Nr5a2^{+/-}$ pancreases under basal conditions and those upregulated in wild-type pancreases were notably reduced 8–24 h after pancreatitis induction; a similar pattern of reduced differences between $Nr5a2^{+/-}$ and wild-type pancreases was observed for the downregulated genes. The expression of a random set of genes was unaffected (Extended Data Fig. 5a). Consistently, although there was a strong upregulation of AP-1 at 8 h after induction of pancreatitis in mice of both genotypes, persistent AP-1 upregulation at 24–48 h was observed only in $Nr5a2^{+/-}$ mice (Extended Data Fig. 5b). These results indicate that *Nr5a2* haploinsufficiency mimics acute pancreatitis at the transcriptome level.

The repeated caerulein dosing required to induce pancreatitis hampers the interpretation of dynamic acute signalling and transcriptional responses. Therefore, we also analysed the effects of a single dose of caerulein that did not induce pancreatitis (Extended Data Fig. 6a). JUN,

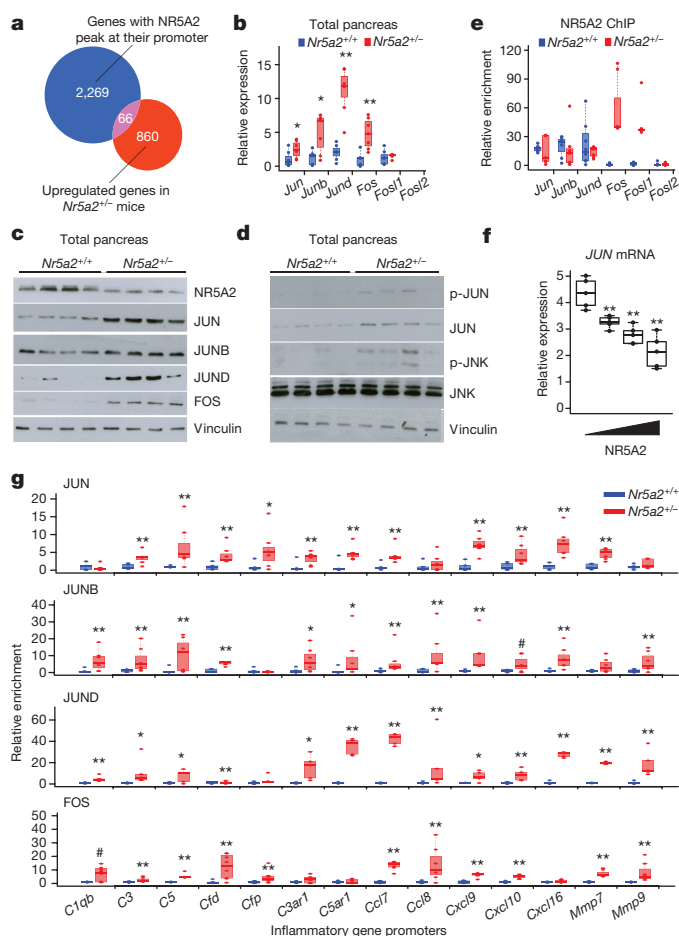


Figure 2 | AP-1 components are upregulated and bind to the promoter of inflammatory genes in *Nr5a2*^{+/-} pancreases. **a**, A total of 926 genes are upregulated in *Nr5a2*^{+/-} pancreases. In ChIP-seq experiments using normal pancreas cells, 2,269 genes have an NR5A2 peak at their promoter. A minor fraction of the promoters of genes upregulated in *Nr5a2*^{+/-} pancreases (66 out of 926) also display NR5A2 peaks at their promoters in normal pancreas cells. **b**, qRT-PCR of AP-1 component expression in an independent group of wild-type and *Nr5a2*^{+/-} mice (*n* = 7 per group). **c**, **d**, Western blots showing NR5A2, AP-1, p- JUN and p- JNK expression in wild-type and *Nr5a2*^{+/-} pancreases (*n* = 4 per group). **e**, NR5A2 enrichment at AP-1 gene promoters revealed by ChIP-qPCR (*n* = 7 per group). **f**, qRT-PCR of JUN expression in HEK293 cells upon transfection of a plasmid coding for NR5A2, showing reduced *Jun* mRNA (mean of five independent experiments). **g**, ChIP-qPCR of the occupancy of inflammatory gene promoters by AP-1 (JUN, JUNB, JUND and FOS) in wild-type and *Nr5a2*^{+/-} pancreases (*n* ≥ 5 per group). At least two independent experiments were performed in all cases. In **b**, **e**, **f** and **g**, one-sided Mann-Whitney *U* test; **P* < 0.05, ***P* < 0.01.

FOS, JUND, FOSL1 and FOSL2 (also known as FRA2) were upregulated to a similar extent in both wild-type and *Nr5a2*^{+/-} pancreases 30–60 min after caerulein administration, preceding STAT3 phosphorylation (Extended Data Fig. 6b). We then analysed the expression of a subset of the genes differentially overexpressed in *Nr5a2*^{+/-} pancreases under basal conditions. By 30–60 min, one dose of caerulein was sufficient to promote an inflammatory profile in wild-type mice; this profile closely resembled that of *Nr5a2*^{+/-} pancreases. A complete resolution of this expression profile occurred in wild-type mice by 12 h (Fig. 3a, b). To determine whether these are epithelial-cell-autonomous effects, primary acini from wild-type and *Nr5a2*^{+/-} mice were treated with vehicle or caerulein for 24 h. qRT-PCR analysis confirmed that under control conditions *Nr5a2*^{+/-} acini express higher levels of inflammatory genes than wild-type acini, and that these differences were abolished upon caerulein treatment (Extended Data Fig. 6c).

These findings further support the notion that *Nr5a2*^{+/-} acini display a transcriptional pre-inflammatory phenotype similar to that of caerulein-treated wild-type acini.

A large fraction of inflammatory gene promoters contain putative NR5A2 binding sites that are not occupied in normal pancreas (Fig. 2a, data not shown). Accordingly, we performed ChIP-qPCR on the promoter of bona fide NR5A2 target differentiation-related genes (that is, those encoding digestive enzymes) and of inflammatory genes upregulated in *Nr5a2*^{+/-} mice. In untreated wild-type mice NR5A2 was observed to bind at the promoter of differentiation genes, but not at the promoter of inflammatory genes (Fig. 3c). However, in untreated *Nr5a2*^{+/-} mice, the binding of NR5A2 to differentiation gene promoters was reduced and binding to inflammatory gene promoters was increased. We designate this relocation of NR5A2 between gene sets as the ‘NR5A2 transcriptional switch’. A similar transcriptional switch occurred in wild-type mice 30 min after 1 dose of caerulein and the genomic distribution of NR5A2 was restored 12 h later (Fig. 3d), supporting its physiological relevance. NR5A2 can interact with JUN *in vitro*¹³, and we found that both proteins co-immunoprecipitated in the pancreases of untreated *Nr5a2*^{+/-} mice and in wild-type mice 1 h after caerulein administration, but not in untreated wild-type mice (Fig. 3e). Using sequential ChIP-qPCR, NR5A2 and JUN were detected on the same immunoprecipitated chromatin regions at the promoters of *C1qb*, *Ccl7* and *Ccl8* in untreated *Nr5a2*^{+/-} mice and in wild-type mice 1 h after caerulein administration, supporting the proposition that JUN and AP-1 cooperate in producing the NR5A2 transcriptional switch (Fig. 3f and Extended Data Fig. 7).

NR0B2 is an NR5A2 co-repressor and target gene¹⁴ that is highly expressed in acinar cells, shows reduced expression in *Nr5a2*^{+/-} pancreases and is dynamically regulated on caerulein administration (Extended Data Fig. 8a–e). In humans, *NR0B2* mRNA expression was significantly higher in NR5A2^{high} pancreases (*P* = 1.4 × 10⁻⁷) and NR5A2 and NR0B2 levels were positively correlated with one another (*R*² = 0.312) (Extended Data Fig. 8f), which suggests that NR0B2 contributes to the haploinsufficient phenotype. Under basal conditions in wild-type mice, NR0B2 was absent from the promoter of differentiation and inflammatory genes but it was enriched in the promoter of *Jun*, *Junb* and *Jund* (Extended Data Fig. 8g). *Nr5a2*^{+/-} pancreases displayed reduced NR0B2 levels, lower occupancy of AP-1 promoters by NR0B2, reduced binding of NR5A2 at the *Nr0b2* promoter and reduced complexing of NR5A2 with NR0B2 (Extended Data Fig. 8c, g–i), which suggests that NR0B2 ordinarily represses AP-1 expression. We validated the 266-6 mouse acinar cell line as a model to assess the effects of caerulein on AP-1 and inflammatory genes (Extended Data Fig. 9a–c). On expression of NR0B2, *Jun* mRNA—but no inflammatory transcript—was reduced and NR0B2 knockdown modestly increased NR5A2 occupancy of inflammatory gene promoters (Extended Data Figs 9d, e). The effects of NR5A2 knockdown on JUN and inflammatory gene expression were abrogated by NR0B2 overexpression (Extended Data Fig. 9f), supporting the notion that NR5A2 modulates AP-1 expression in part through NR0B2 downregulation.

AP-1 upregulation, increased binding to inflammatory gene promoters in *Nr5a2*^{+/-} mice and the interaction of JUN and NR5A2 all suggest a crucial involvement of JUN in the basal pre-inflammatory state. *Jun* deletion in *Nr5a2*^{+/-} pancreases rescued the upregulation of AP-1 and inflammatory transcripts, as well as NR5A2 binding to AP-1 and inflammatory gene promoters, without affecting NR5A2 expression (Fig. 4a–d). On induction of acute pancreatitis, *Nr5a2*^{+/-} mice in which the *Jun* gene has been deleted in the pancreas (*Nr5a2*^{+/-}; *Jun*Δ*P*) showed reduced damage when compared with control *Nr5a2*^{+/-} mice (Fig. 4e, f). The normalization of the dynamic expression of AP-1 components during pancreatitis in *Nr5a2*^{+/-}; *Jun*Δ*P* pancreases suggests a critical role for JUN in the phenotype of *Nr5a2*^{+/-} mice. Immunohistochemical analysis showed that the downregulation of JUN occurred selectively in acinar cells (Fig. 4g and Extended Data Fig. 10). Taken together, these results indicate that *Jun* is required to generate the pre-inflammatory state observed in *Nr5a2*^{+/-} pancreases.

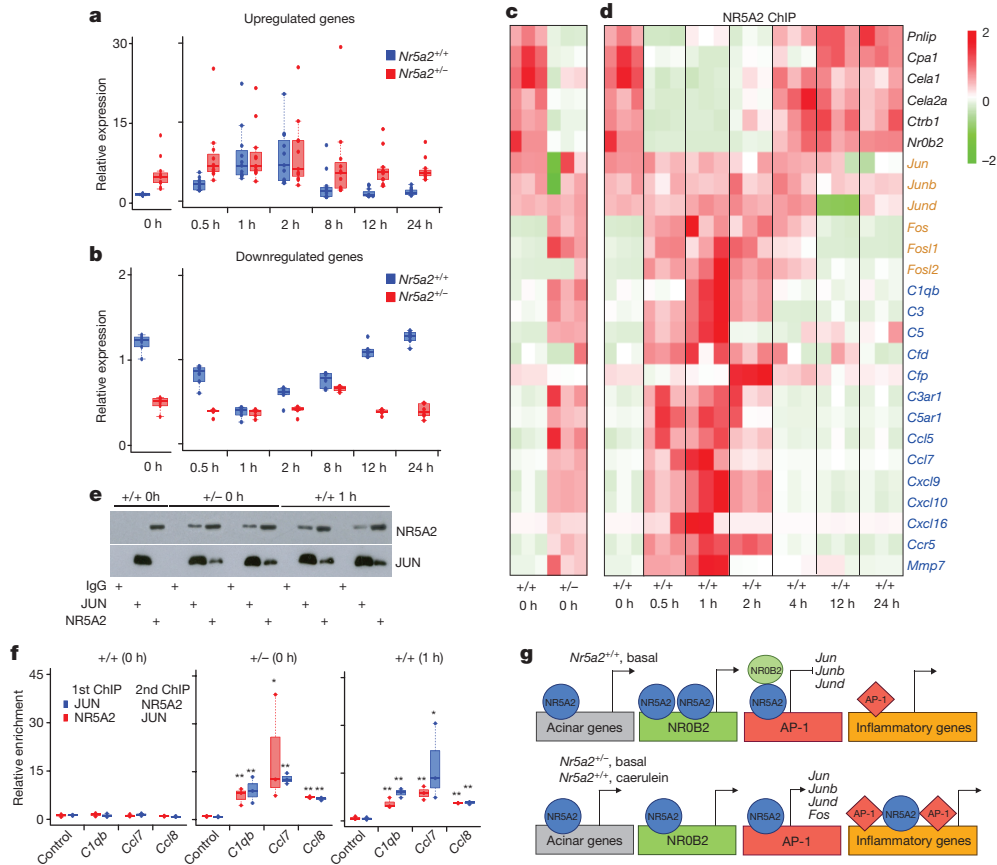


Figure 3 | The NR5A2 transcriptional switch. **a, b**, Dynamic gene expression ($Nr5a2^{+/-}$ versus $Nr5a2^{+/+}$) after one dose of caerulein, shown using qRT-PCR. Data refer to basal values in wild-type pancreases ($n = 4$ per group; two independent experiments). **c**, ChIP-qPCR showing differential promoter occupancy by NR5A2 under basal conditions ($n = 3$ per group). **d**, ChIP-qPCR showing NR5A2 switching from the promoter of pancreatic genes to the promoter of inflammatory genes after one caerulein dose in wild-type mice (black, pancreatic genes; orange, AP-1 genes; blue, inflammatory genes) ($n = 3$ per group; two independent experiments). **e**, Co-immunoprecipitation and western blot showing that NR5A2 and JUN are part of the same complex in $Nr5a2^{+/-}$ pancreases under basal conditions and in wild-type mouse pancreases after one dose of caerulein, but not in wild-type mouse pancreases under basal conditions (at least two independent experiments). **f**, Sequential ChIP-qPCR of JUN-NR5A2 and NR5A2-JUN to assess promoter binding in wild-type pancreases under basal conditions, and 1 h after caerulein dosing

In homeostatic conditions, tissue inflammation is suppressed. However, a direct link between differentiation and inflammatory programmes has not yet been proposed. Here, we demonstrate that NR5A2 is critical in restraining inflammation in normal mouse pancreas cells. Constitutive loss of one $Nr5a2$ allele produces a pre-inflammatory state that explains how haploinsufficiency primes tissue for damage and delays recovery, which may contribute to accelerated tumorigenesis¹¹. This pre-inflammatory state is mediated by JUN phosphorylation and stabilization, which are hallmarks of JUN activation¹⁵. In $Nr5a2^{+/-}$ mice, low NR5A2 and NR0B2 expression probably determine AP-1 dysregulation, which contributes to inflammatory gene expression, as occurs on induction of pancreatitis, (Fig. 3g). In the pancreas, AP-1 is pro-inflammatory; this is unlike the situation found in the skin, in which *Jun* and *Junb* deletion in keratinocytes induces inflammatory phenotypes¹⁶. Our results, therefore, support the notion that the effects of AP-1 are context-dependent and tissue-specific^{17,18}. The output of the interaction of NR5A2, NR0B2 and AP-1 with gene regulatory elements is likely to be modulated by post-transcriptional modifications and chromatin accessibility: in keratinocytes, the coordinated regulation of polycomb-group and AP-1 proteins ensures canonical expression of epidermal genes during differentiation¹⁹.

(see Extended Data Fig. 7) ($n = 3$ pools of 3 pancreases). One-sided Mann-Whitney U test; * $P < 0.05$, ** $P < 0.01$. **g**, Proposed model of the NR5A2 transcriptional switch. Under basal conditions in wild-type mice, NR5A2 is bound to acinar gene promoters as well as to the promoter of *Nr0b2*. In this condition, AP-1 proteins show weak binding to inflammatory gene promoters. By contrast, in untreated $Nr5a2^{+/-}$ mice, and in wild-type mice that have received caerulein, NR5A2 is weakly bound to the promoter of acinar genes but shows increased binding to the promoters of *Fos*, *Fos1* and inflammatory genes; AP-1 proteins also show increased binding to these promoters. In wild-type mice dosed with caerulein, there is a transient redistribution of NR5A2 to AP-1 genes, and of AP-1 proteins to inflammatory genes. NR0B2 levels are reduced in untreated $Nr5a2^{+/-}$ mice and in wild-type mice that have received caerulein. This is accompanied by reduced binding to AP-1 promoters, which suggests that NR0B2 participates in the regulation of AP-1 gene expression.

We find chemokines and complement components among the inflammatory genes most prominently upregulated in $Nr5a2^{+/-}$ pancreases. The control of inflammation from epithelial cells at the level of chemotactic stimuli suggests that leukocyte migration to tissues generates the local upregulation of cytokines, such as IL1, IL6 and TNF, which then contribute to amplifying and prolonging the inflammatory response²⁰. The findings in $Nr5a2^{+/-}$ pancreases indicate that inflammation is actively repressed in normal epithelial cells, and that the genetic pre-inflammatory phenotype mimics the molecular events associated with response to pharmacological (such as caerulein) and environmental stimuli. Indeed, both conditions are associated with a switch in the chromatin distribution of NR5A2, which shifts from the promoters of pancreatic differentiation genes to those of inflammatory genes. Our findings in mice are relevant to human pancreatitis and PDAC, as shown by shared transcriptomic changes that indicate a pre-inflammatory state in the pancreas of human subjects with low NR5A2 mRNA levels and by the association of this pre-inflammatory state with low levels of NR5A2 and NR0B2. Although additional work is needed to establish the functional consequences of carrying PDAC-risk alleles at chr1q32.1, our results suggest that the underlying biology at this locus may involve negative regulation of NR5A2 expression.

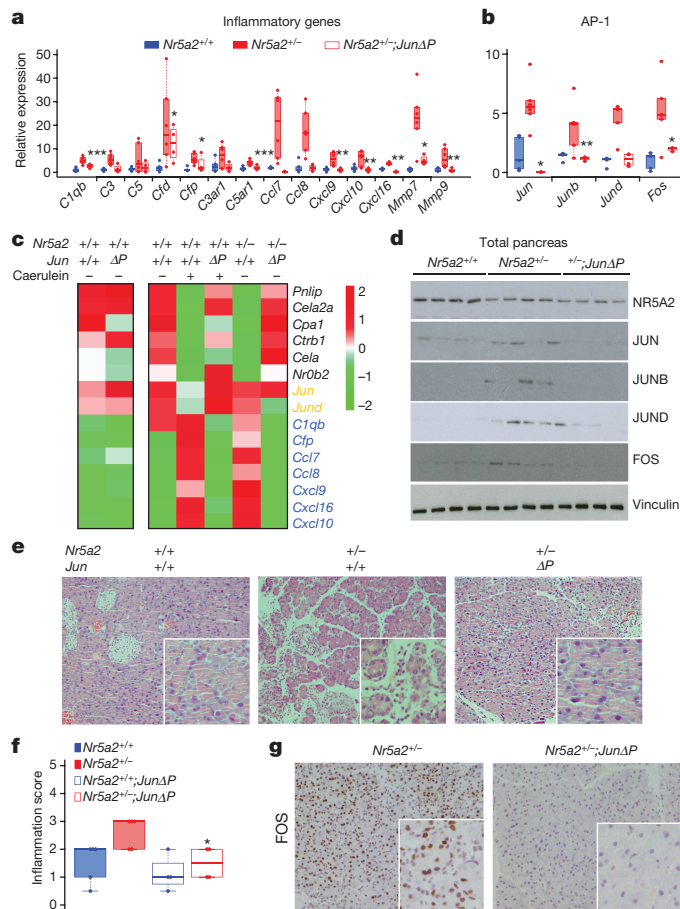


Figure 4 | Pancreatic deletion of *Jun* rescues the pancreatic defect of *Nr5a2*^{+/-} mice. **a**, qRT-PCR analysis of inflammatory gene (a) and AP-1 (b) transcripts in the pancreas of wild-type, *Nr5a2*^{+/-} and *Nr5a2*^{+/-};*Jun*Δ*P* mice; **a** and **b** are shown relative to basal values in wild-type mice ($n \geq 4$). **c**, ChIP-qPCR shows that the NR5A2 transcriptional switch is reversed on the deletion of *Jun* in the pancreas ($n =$ pool of 3 pancreases). This experiment was performed once. **d**, Western blots showing the expression of NR5A2 and AP-1 in *Nr5a2*^{+/+}, *Nr5a2*^{+/-} and *Nr5a2*^{+/-};*Jun*Δ*P* pancreases ($n = 4$ per group). **e**, Histology of *Nr5a2*^{+/+}, *Nr5a2*^{+/-} and *Nr5a2*^{+/-};*Jun*Δ*P* pancreases 48 h after induction of acute pancreatitis shows that *Jun* deletion rescues the excessive damage caused by *Nr5a2* haploinsufficiency ($n \geq 4$ per group). All experimental data were obtained in a single experiment. **f**, Inflammation scores corresponding to the experiment in **e** ($n \geq 4$ per group), plus scores from *Nr5a2*^{+/+} mice with a *Jun* deletion. **g**, Immunohistochemistry of FOS in *Nr5a2*^{+/-} and *Nr5a2*^{+/-};*Jun*Δ*P* pancreases 48 h after induction of acute pancreatitis ($n = 4$ per group; representative results of one pancreas). In **a**, **b** and **f**, one-sided Mann-Whitney *U* test; * $P < 0.05$, ** $P < 0.01$.

Online Content Methods, along with any additional Extended Data display items and Source Data, are available in the online version of the paper; references unique to these sections appear only in the online paper.

Received 7 July 2016; accepted 15 January 2018.

Published online 14 February 2018.

- Karin, M. & Clevers, H. Reparative inflammation takes charge of tissue regeneration. *Nature* **529**, 307–315 (2016).
- Grivennikov, S. I., Greten, F. R. & Karin, M. Immunity, inflammation, and cancer. *Cell* **140**, 883–899 (2010).
- Crusz, S. M. & Balkwill, F. R. Inflammation and cancer: advances and new agents. *Nat. Rev. Clin. Oncol.* **12**, 584–596 (2015).
- Stein, S. & Schoonjans, K. Molecular basis for the regulation of the nuclear receptor LRH-1. *Curr. Opin. Cell Biol.* **33**, 26–34 (2015).
- Mamrosh, J. L. et al. Nuclear receptor LRH-1/NR5A2 is required and targetable for liver endoplasmic reticulum stress resolution. *eLife* **3**, e01694 (2014).
- Holmstrom, S. R. et al. LRH-1 and PTF1-L coregulate an exocrine pancreas-specific transcriptional network for digestive function. *Genes Dev.* **25**, 1674–1679 (2011).

- Molero, X. et al. Gene expression dynamics after murine pancreatitis unveils novel roles for Hnf1 α in acinar cell homeostasis. *Gut* **61**, 1187–1196 (2012).
- Hale, M. A. et al. The nuclear hormone receptor family member NR5A2 controls aspects of multipotent progenitor cell formation and acinar differentiation during pancreatic organogenesis. *Development* **141**, 3123–3133 (2014).
- Petersen, G. M. et al. A genome-wide association study identifies pancreatic cancer susceptibility loci on chromosomes 13q22.1, 1q32.1 and 5p15.33. *Nat. Genet.* **42**, 224–228 (2010).
- Amundadottir, L. T. Pancreatic cancer genetics. *Int. J. Biol. Sci.* **12**, 314–325 (2016).
- Flández, M. et al. *Nr5a2* heterozygosity sensitises to, and cooperates with, inflammation in *KRAS*^{G12V}-driven pancreatic tumourigenesis. *Gut* **63**, 647–655 (2014).
- Zhang, M. et al. Characterizing *cis*-regulatory variation in the transcriptome of histologically normal and tumour-derived pancreatic tissues. *Gut* <http://dx.doi.org/10.1136/gutjnl-2016-313146> (2017).
- Huang, S. C., Lee, C. T. & Chung, B. C. Tumor necrosis factor suppresses NR5A2 activity and intestinal glucocorticoid synthesis to sustain chronic colitis. *Sci. Signal.* **7**, ra20 (2014).
- Oiwa, A. et al. Synergistic regulation of the mouse orphan nuclear receptor SHP gene promoter by CLOCK-BMAL1 and LRH-1. *Biochem. Biophys. Res. Commun.* **353**, 895–901 (2007).
- Papavassiliou, A. G., Chavrier, C. & Bohmann, D. Phosphorylation state and DNA-binding activity of c-Jun depend on the intracellular concentration of binding sites. *Proc. Natl Acad. Sci. USA* **89**, 11562–11565 (1992).
- Schönthaler, H. B., Guinea-Viniegra, J. & Wagner, E. F. Targeting inflammation by modulating the Jun/AP-1 pathway. *Ann. Rheum. Dis.* **70**, i109–i112 (2011).
- Shaulian, E. & Karin, M. AP-1 as a regulator of cell life and death. *Nat. Cell Biol.* **4**, E131–E136 (2002).
- Eferl, R. & Wagner, E. F. AP-1: a double-edged sword in tumorigenesis. *Nat. Rev. Cancer* **3**, 859–868 (2003).
- Ezhkova, E. et al. Ezh2 orchestrates gene expression for the stepwise differentiation of tissue-specific stem cells. *Cell* **136**, 1122–1135 (2009).
- Headland, S. E. & Norling, L. V. The resolution of inflammation: principles and challenges. *Semin. Immunol.* **27**, 149–160 (2015).

Supplementary Information is available in the online version of the paper.

Acknowledgements We thank O. Domínguez, J. Herranz, T. Lobato, L. Martínez, and Y. Cecilia, as well as members of the CNIO core facilities, Epithelial Carcinogenesis Group, and Genes, Development and Disease Group; L. Montuenga, C. Rodríguez-Ortigosa, B. Bréant and cited investigators for providing antibodies; and E. Batlle and P. Muñoz-Cánoves for critical comments. This study used the high-performance computational capabilities of the Biowulf Linux cluster (<https://hpc.nih.gov/>). The content of this publication does not necessarily reflect the views or policies of the Department of Health and Human Services, US National Institutes of Health (NIH), nor does mention of trade names, commercial products or organizations imply endorsement by the US government. This work was supported in part by grants SAF2011-29530 and SAF2015-70553-R from the Ministerio de Economía y Competitividad (co-funded by the ERDF-EU), RTICC from the Instituto de Salud Carlos III (RD12/0036/0034, RD12/0036/0050) and grants 256974 and 289737 from the European Union Seventh Framework Program to F.X.R.; grants BFU 2012-40230 and SAF2015-70857 from the Ministerio de Economía y Competitividad (co-funded by the ERDF-EU) and Worldwide Cancer Research (13-0216) to E.F.W.; grants PI12/00815 and PI1501573 from the Fondo de Investigaciones Sanitarias, Instituto de Salud Carlos III, Spain and EUPancreas COST Action BM1204 to N.M.; grant P30CA008748 from the US NIH, National Cancer Institute to S.H.O.; the Intramural Research Program of the NIH, National Cancer Institute; and Mayo Clinic SPORE in Pancreatic Cancer funded by National Cancer Institute grant P50 CA102701. L.T. and T.B. were supported by the Department of Technology, Norwegian University of Science and Technology, the Central Norway Regional Health Authority and by the European Science Foundation. P.M. and I.C. are recipients of Juan de la Cierva and Beca de Formación del Personal Investigador, respectively, from Ministerio de Economía y Competitividad. I.F. is the recipient of a 'Juegaterapia-Armos del CNIO' Postdoctoral Fellowship. F.X.R. acknowledges the support of Asociación Española Contra el Cáncer.

Author Contributions I.C., M.F. and F.X.R. conceived the study. I.C., M.F. and N.d.P. performed animal experiments. I.C., E.C.-d.-S.-P., M.Z. and J.J. conducted bioinformatics analyses. I.C., V.J.S.-A.L. and I.F. conducted *in vitro* studies using mouse cells. S.H.O., J.S., W.R.B., G.M.P. and N.M. provided samples and information on human subjects. W.R.B., G.M.P., N.M. and L.T.A. designed and performed clinical studies, obtained samples and performed human data analysis. I.M., D.M., L.T. and T.B. were involved in data analysis. L.B., K.S. and E.F.W. provided reagents. P.M., L.B., L.T.A. and E.F.W. had critical input into experimental design, data analysis and interpretation. I.C. and F.X.R. wrote the manuscript with contributions of P.M., L.B., L.T.A. and E.F.W. F.X.R. supervised the overall conduct of the study. All authors read and approved the final manuscript.

Author Information Reprints and permissions information is available at www.nature.com/reprints. The authors declare no competing financial interests. Readers are welcome to comment on the online version of the paper. Publisher's note: Springer Nature remains neutral with regard to jurisdictional claims in published maps and institutional affiliations. Correspondence and requests for materials should be addressed to F.X.R. (preal@cnio.es).

Reviewer Information *Nature* thanks F. Greten, R. MacDonald and G. Natoli for their contribution to the peer review of this work.

METHODS

No statistical methods were used to pretermine sample size. The investigators were not blinded to allocation during experiments but were blinded to outcome assessment.

Mice and experimental manipulations. The following mouse strains were used: *Nr5a2*^{+/-} (ref. 21), conditional floxed *Jun*²², conditional floxed *Nr5a2*²³, *Lys*^{cre} (ref. 24), and *Ptf1a*^{cre/+} knock-in mice (a gift from C. V. Wright)²⁵. Pancreas-specific *Nr5a2*-heterozygous and *Jun*-deficient mice were generated by crossing *Nr5a2*^{lox/+} and *Jun*^{lox/lox} mice with *Ptf1a*^{cre/+} mice, respectively. All crosses were maintained in a predominantly C57BL/6 background. Littermate control mice were used. All experiments were performed using 8–14-week-old mice. All animal procedures were approved by local and regional ethics committees (Institutional Animal Care and Use Committee and Ethics Committee for Research and Animal Welfare, Instituto de Salud Carlos III) and performed according to the European Union guidelines. After a mouse was killed by cervical dislocation, the pancreas was removed quickly and placed in buffered formalin for histological analysis or homogenized in denaturing buffer (4 M guanidine thiocyanate, 0.1 M Trizma HCl pH 7.5, 1% 2-mercaptoethanol) for RNA extraction. In addition, a small piece was snap-frozen for protein isolation.

Mild acute pancreatitis was induced by seven injections, given once per hour, of the CCK analogue caerulein (Bachem) at 50 µg kg⁻¹. In brief, animals were weighed before beginning the procedure and caerulein was administered intraperitoneally. Mice were killed by cervical dislocation 8, 24 and 48 h after the first injection. For the single-injection protocol, mice received a single dose of caerulein (50 µg kg⁻¹) administered intraperitoneally. Mice were killed by cervical dislocation at the indicated time points.

The number of mice used in each experiment is shown in the legend of each figure. For most experiments, at least five mice per group were used; if different numbers of mice were included in each group, the lowest number is provided. No specific randomization method was used.

Acinar cell isolation. Acinar cells were isolated by collagenase digestion and maintained at 37 °C in Dulbecco's modified Eagle medium containing 2% bovine serum albumin and 10 mM 4-(2-hydroxyethyl)-1-piperazine ethanesulfonic acid as previously described²⁶. Acini were treated either with caerulein (100 pM) or with saline for 24 h before RNA and protein isolation.

Immunofluorescence and immunohistochemical analyses. Immunofluorescence and immunohistochemical analyses were performed using 3-µm sections of formalin-fixed paraffin-embedded tissues, unless otherwise indicated. After deparaffinization and rehydration, antigen retrieval was performed by boiling in citrate buffer pH 6 for 10 min. For immunofluorescence, the sections were incubated for 45 min at room temperature with 3% BSA, 0.1% Triton X-100–PBS and then with the primary antibody overnight at 4 °C. For double or triple immunofluorescence, the corresponding antibodies were added simultaneously and incubated overnight at 4 °C. Sections were then washed with 0.1% Triton–PBS, incubated with the appropriate fluorochrome-conjugated secondary antibody, and nuclei were counter-stained with DAPI. After washing with PBS, sections were mounted with Prolong Gold Antifade Reagent (Life Technology).

For immunofluorescence quantification of Cd45⁺ cells, fresh-frozen tissues were used. Sections were fixed with 4% paraformaldehyde for 10 min at room temperature with gentle rotation, washed with PBS and incubated with 3% BSA and 0.1% Triton–PBS for 45 min at room temperature, followed by overnight incubation with primary antibodies recognizing PTF1a (gift from B. Bréant, INSERM) and Cd45 (NB110-93609, Novus Biologicals). After washing with PBS, sections were incubated with the appropriate fluorochrome-conjugated secondary antibodies, and nuclei were counter-stained with DAPI. After washing with PBS, sections were mounted as described. Images were analysed with Definiens Developer XD v.2.5 software (Definiens): a script was developed in-house for single-cell segmentation. Afterwards, cells were classified into subtypes by calculating the nuclear and cytoplasmic intensity of the different markers. Owing to the low quantities of marker-positive cells, a picture gallery of all single positives was generated and false-positive images were manually discarded by one of the co-authors (D.M.) for maximum accuracy; this process was performed in a blinded fashion. There were no differences between wild-type and *Nr5a2*^{+/-} mice, and only the raw uncurated results are shown in Extended Data Fig. 2e.

For immunohistochemical analyses, after antigen retrieval endogenous peroxidase was inactivated with 3% H₂O₂–methanol for 30 min at room temperature. Sections were incubated with 2% BSA–PBS for 1 h at room temperature, and incubated with the primary antibody. After washing, the Envision secondary reagent (DAKO) was added for 40 min at room temperature and sections were washed three times with PBS. 3,3'-Diaminobenzidine tetrahydrochloride (DAB) was used as a chromogen. Sections were lightly counterstained with haematoxylin, dehydrated and then mounted. A non-related IgG was used as a negative control.

To identify ductal cells, the *Dolichos biflorus* agglutinin (DBA)–streptavidin visualization system was used (Discovery DAB Map Kit, RUO, Ventana). Sections were incubated with biotinylated DBA (1:1000; Vector Laboratories B-1035), washed and incubated with streptavidin–peroxidase. Reactions were developed using DAB. Histological images were acquired with a Nikon TE2000 microscope and the percentage of cells expressing DBA was quantified.

To quantify Cd45⁺ leukocytes using immunohistochemistry, an automated immunostaining platform was used (Ventana Discovery XT, Roche). Antigen retrieval was first performed with boiling citrate buffer pH 6.0; endogenous peroxidase was blocked and slides were incubated with rat monoclonal anti-CD45 (5C16, 1:500; Novus Biologicals, NB110-93609). Slides were incubated with the corresponding secondary antibodies (biotinylated rabbit anti-rat Ig, Vector Labs) and visualization systems (OmniRabbit, Ventana, Roche) conjugated with horseradish peroxidase. Immunohistochemical reactions were developed using DAB and nuclei were counterstained with haematoxylin. Finally, the slides were dehydrated, cleared and mounted for microscopic evaluation. Whole digital slides were acquired with a scanner (Axio Scan Z1, Zeiss) and images captured with Zen Software (Zeiss). Image analysis and quantification were performed using with the AxioVision software package (Zeiss). After selecting regions of interest, areas were selected for quantification and exported as subset TIFF images. Images with artefactual staining or cutting artefacts were eliminated. Afterwards, the images from all slides were chosen for automatic quantification (AxioVision 4.6, Zeiss) using a script for each antibody. For Cd45 quantification, positivity was evaluated in one phase (phase 1, positive) and compared with total tissue area (phase 2). The output results were then exported as Excel files with scoring data for each TIFF file. Data obtained were then compiled and appropriately assessed.

Histological scoring of mouse pancreases. Inflammation-related histological parameters (oedema, inflammatory cell infiltration and acino-ductal metaplasia) were scored blindly according to the grade of severity (0–3).

Flow cytometry analysis of inflammatory cells. In brief, mouse pancreases were injected *in situ* with collagenase P (1 mg/mL) (Roche), transferred to cold collagenase and minced. After incubating at 37 °C for 20 min with mild shaking, collagenase was inactivated with 5% cold FBS in HBSS and the pancreas was disaggregated and filtered twice through a 70-µm strainer. After centrifugation for 2 min at 300g and resuspension (2% chelated FBS, 2 mM EDTA, supplemented with DNase in HBSS) (Ambion), live cells were counted, incubated with blocking buffer and subsequently with primary antibody for 1 h at room temperature. Cell suspensions were analysed through a FACS ARIA IIu sorter coupled to a LSR Fortessa analyser with 10 different markers (Fig. 1f and Extended Data Fig. 2d). Mice with low counts of total live cells were not considered in the analyses. For each condition, ≥ 5 mice were used.

RNA-seq and data processing in mouse cells. Total pancreatic RNA was isolated using guanidine thiocyanate, followed by acid phenol–chloroform extraction. RNA integrity numbers ranged from 6.6 to 9.2, when assayed by laboratory chip technology on an Agilent 2100 Bioanalyzer. PolyA⁺ RNA was extracted and randomly fragmented, converted to double stranded cDNA and processed through subsequent enzymatic treatments of end-repair, dA-tailing and ligation to adapters according to Illumina's 'TruSeq RNA Sample Preparation Guide' (Part # 15008136 Rev. A; for samples Big104, Big90, Big92, Big18, Big277, Big278, Big33, Big87, Big94, Big113, Big17, Big86) or Illumina's 'TruSeq RNA Sample Preparation v.2 Protocol' (Part # 15026494 Rev. C; for samples Big408, Big409, Big410, Big416, Big417, Big423, Big454, Big459, Big461, Big465, Big467 and Big470). The adaptor-ligated library was completed by limited-cycle PCR with Illumina PE primers (10 cycles, or 8 cycles for samples using the v.2 protocol). The resulting purified cDNA library was applied to an Illumina flow cell for cluster generation (TruSeq cluster generation kit v.5) and sequenced on the Genome Analyzer IIx with SBS TruSeq v.5 reagents, according to the manufacturer's protocols. Three pancreases were analysed for each genotype (wild type or *Nr5a2*^{+/-}) and condition (baseline, 8 h, 24 h and 48 h after pancreatitis induction).

Image analysis and per-cycle base-calling were performed with Illumina real time analysis software (RTA1.13). Conversion to FASTQ read format with the ELAND algorithm (v.2e) was performed with CASAVA-1.8 (Illumina). These files contain only reads that passed 'chastity' filtering (tagged with an 'N', for *NOT filtered* in the sequence identifier line). Quality check was done using fastqc (v.0.9.4, Babraham Bioinformatics) and raw reads were aligned to the NCBI37/mm9 version of the mouse genome. Tophat5 (v.2.0.4) was used for alignment with the following parameters: –bowtie1, –max-multihits 5, –genome-read-mismatches 1 –segment-mismatches 1 –segment-length 20 –splice-mismatches 0. Gene expression was quantified with cufflinks (v.2.0.2) with the following parameters: -N, -u. Further, gene expression values were normalized for library size with cuffnorm, with the following parameters: -o -L –library-norm-method classic-fpkm. Cuffdiff was used to find differential gene expression among conditions with the following parameters: -num-threads 16, -multi-read-correct,

-frag-bias-correct. Differentially expressed genes were considered with q -value of less than 0.05 (adjusted P values found using an optimized false discovery rate approach).

ChIP-seq data processing. SRR389293 and SRR389294 images were downloaded from the Gene Expression Omnibus website⁶. The quality check was performed using fastqc (v.0.9.4, Babraham Bioinformatics). ChIP-seq reads were aligned to the mouse reference genome NCBI37/mm9 (accessed July 2007) with Burrows-Wheeler Aligner (bwa, v.0.5.9-r16) allowing 0–1 mismatches. Uniquely aligned reads were converted to BED format. Macs14 (v.1.4.1 20110622) was used for peak calling using the following parameters: -t SRR389393, -c SRR389294 -f BED -g mm. Other parameters were used as default. PeakAnalyzer 1.4 was used to annotate NR5A2 binding sites. Motif enrichment was identified with the MEME suite using the default parameters. Reads were directionally extended to 300 bp and, for each base pair in the genome, the number of overlapping sequence reads was determined and averaged over a 10-bp window to create a wig file to visualize the data in the University of California Santa Cruz (UCSC) genome browser.

Principal component analysis. The Pearson correlation was calculated from the expression value (expressed as fragments per kilobase of transcript per million mapped reads) of each gene for each sample by using the 'cor' command in R (<https://www.r-project.org/>). Principal component analysis was performed using the 'prcomp' command in R, from the correlation value of each sample.

GSEA. The list of genes was ranked by the 't-stat' statistical value from the cuffdiff output file. The list of pre-ranked genes was then analysed with GSEA for Gene Ontology (GO) database. Significantly enriched GO terms were identified using a false discovery rate q value of less than 0.25. The analyses were carried out as defined in http://www.broadinstitute.org/gsea/doc/GSEAUserGuideFrame.html?Interpreting_GSEA.

Singular enrichment analysis. The differentially expressed gene sets were computed at the molecular signature dataset of GSEA, using the Biological Processes dataset.

Human transcriptome RNA-seq analysis. Histologically normal fresh frozen pancreatic tissue samples ($n = 95$) from patients with pancreatic cancer ($n = 79$) (Mayo Clinic; Memorial Sloan Kettering Cancer Center) or from organ donors ($n = 16$) (Penn State College of Medicine and Gift of Life Donor Program) were used. Histological review was performed at each participating institution. Subjects of self-reported non-European ancestry and those with a history of neo-adjuvant therapy before surgery were excluded from the study. All relevant ethical regulations were followed. The project was approved by the Institutional Review Boards of Memorial Sloan Kettering Cancer Center, the Mayo Clinic and Georgetown Universities; exemption for the work with human tissue samples at NIH was approved by the NIH Office of Human Subject Research. Human samples were anonymized. Written informed consent was obtained from human subjects.

RNA was isolated with the mirVana kit (Ambion). Samples with RNA integrity numbers of greater than 7.5 (1 μ g) were subject to massive parallel paired-end sequencing on the Illumina HiSeq2000 sequencing platform (TruSeq v.3 chemistry) at the CCR Sequencing Facility of the National Cancer Institute, as previously described²⁷. Read alignment (MapSplice²⁸) and gene expression quantification (in transcripts per million mapped reads, RSEM v.1.2.14^{12,29}) was performed using settings and reference data published by The Cancer Genome Atlas University of North Carolina pipeline (https://webshare.bioinf.unc.edu/public/mRNAseq_TCGA/, UNC_mRNAseq_summary.pdf) and the 'UCSC gene' track (hg19/GRCh37) for gene annotation. We compared human samples in the top and bottom quartile of NR5A2 mRNA levels for expression of genes identified as differentially expressed in the two mouse strains (\log_2 -fold change >1 or <-1) and a set of random genes; only those genes for which a bona fide orthologue was found in the human genome were included (upregulated, $n = 718$; and downregulated, $n = 64$). A random list of genes was used for comparison ($n = 173$). Logistic regression models based on upper quantile normalized transcripts per million mapped reads expression values were conducted using R and Bioconductor with adjustments for age, gender and study.

Protein expression-quantitative trait locus analysis. Protein expression-quantitative trait locus analysis was conducted using human PDAC tissue samples from patients of European ancestry, by assessing NR5A2 protein levels in formalin-fixed paraffin-embedded tissue samples ($n = 110$) on tissue microarrays generated at the Mayo Clinic. Immunohistochemistry was performed with rabbit polyclonal anti-NR5A2 antibodies (HPA005455, Sigma-Aldrich) at 1:300 dilution. NR5A2 staining was scored based on intensity (on a scale from 0–3: 0, negative; 1, weak; 2, positive; and 3, strong) and the proportion of reactive cells (0–100%). Histocore was calculated as staining intensity \times percentage of cells. When more than one core was available from a given tumour, the mean score was used. TaqMan genotyping for the single nucleotide polymorphism marking the PDAC risk locus on chr1q32.1 in NR5A2 (rs3790844; genotyping assay: C__27483560_10, Thermo Fisher Scientific) was performed on blood DNA from the same patients. Protein

expression-quantitative trait loci were assessed by linear regression for additive genetic effects on NR5A2 expression based on mean histocore and quantiles of mean histocore (group 1, histocore of less than 120; group 2, histocore of 120 to 149; group 3, histocore of 150 to 169; group 4, histocore of 170 to 209; and group 5 histocore of 210 and above) with adjustments for age, gender, body mass index and tissue microarray slide. Comparison of genotypes and NR5A2 expression was performed using mean histocore quantiles. The Institutional Review Boards of the participating institutions approved the project.

Quantitative RT-PCR. Total RNA was treated with DNase I (Ambion) for 30 min at 37 °C and cDNAs were prepared according to the manufacturer's specifications, using the TaqMan reverse transcription reagents (Applied Biosystems, Roche). qRT-PCR analysis was performed using the SYBR Green PCR master mix and an ABI PRISM 7900HT instrument (Applied Biosystems). The sequence of the primers used is provided in Supplementary Table 4. Expression levels were normalized to endogenous *Hprt* mRNA levels using the $\Delta\Delta C_t$ method. The results shown are representative of at least four biological replicates.

Immunoprecipitation and western blotting. For immunoprecipitation of proteins from fresh total pancreas lysates, a piece of mouse pancreas was isolated and minced in 50 mM Tris-HCl pH 8, 150 mM NaCl, 5 mM EDTA, 0.5% NP-40 containing 3 \times phosphatase inhibitor cocktail (Sigma-Aldrich) and 3 \times EDTA-free complete protease inhibitor cocktail (Roche). Lysates were briefly sonicated until the protein solution was clear, cleared for 10 min at 11,000 r.p.m. at 4 °C and then the supernatant was recovered.

Antibody-coated protein A or protein G dynabeads (Life Technology) were used for immunoprecipitation. In brief, beads were washed three times with PBS and incubated with anti-NR5A2 or normal goat IgG overnight at 4 °C. After washing three times with PBS and twice with coupling buffer (27.3 mM sodium tetraborate, 72.7 mM boric acid), the dry beads were incubated overnight at 4 °C in freshly prepared 38 mM dimethyl pimelimidate dihydrochloride in 0.1 M sodium tetraborate. Afterwards, beads were washed three times with coupling buffer and once with 1 M Tris pH 9. Then, 1 ml of the Tris solution was added to the beads and incubated for 10 min at room temperature with rotation to block amino groups and stop crosslinking. Finally, beads were washed three times with storage buffer (6.5 mM sodium tetraborate/boric acid) and stored at 4 °C until used. Protein lysates (1–5 mg, cells; 10–15 mg, tissues) were then incubated overnight at 4 °C with antibody-coated dynabeads (Thermo Fisher Scientific). Bound immune complexes were washed twice with lysis buffer containing NP-40, and then eluted by boiling in 2 \times Laemmli buffer (10% glycerol, 2% sodium dodecyl sulphate and 0.125 M Tris-HCl pH 6.8) for 5 min.

For co-immunoprecipitation from transfectants, HEK293 cells transfected with the corresponding plasmids were lysed in 50 mM Tris-HCl pH 8, 150 mM NaCl, 5 mM EDTA, 0.5% NP-40 for 30 min at 4 °C. After a brief sonication, cells were cleared by centrifugation for 10 min at 11,000 r.p.m. and the supernatant was recovered. Lysates were pre-cleared with protein A- or protein G-agarose beads and 2 μ g of normal rabbit IgG (Sigma-Aldrich) and then immunoprecipitated with anti-Flag-M2 affinity gel (A2220), EZview Red anti-HA (E6779) (Sigma-Aldrich) for 2 h at 4 °C. The immune complexes were then pelleted by centrifugation and washed twice in NP-40 lysis buffer for 10 min at 4 °C. After washing, 2 \times Laemmli buffer was added and a fraction of the material eluted by boiling was loaded onto a SDS-PAGE and processed for western blotting. For immunoprecipitation with anti-NR5A2, antibody (2 μ g) was added and incubated overnight.

For western blotting, proteins were extracted from pancreatic tissue, isolated acinar cells or cultured cells using either Laemmli buffer or lysis buffer (50 mM Tris-HCl pH 8, 150 mM NaCl, 5 mM EDTA and 0.5% NP-40) supplemented with protease inhibitor and phosphatase inhibitor cocktails. Protein concentration was measured using the BCA reagent (Biorad), or extrapolated when using Laemmli lysis buffer. Proteins were resolved by either by standard SDS-PAGE or 4–20% TGX pre-cast gels (Biorad) and transferred onto nitrocellulose membranes. The antibodies used are listed in Life Sciences Reporting Summary. Densitometry analysis of digitalised western blotting images was performed using Fiji software (NIH).

ChIP. Pancreas tissue was minced, washed with cold PBS supplemented with 3 \times protease and phosphatase cocktail inhibitors, and then fixed with 1% formaldehyde for 20 min at room temperature. Glycine was added to a final concentration of 0.125 M for 5 min at room temperature. The fixed tissue was soaked in SDS buffer (50 mM Tris pH 8.1, 100 mM NaCl, 5 mM EDTA and 0.5% SDS) and homogenized using a douncer. The supernatant was collected after centrifugation and the chromatin was sonicated with a Covaris instrument for 40 min (20% duty cycle; 10% intensity; 200 cycle), yielding DNA fragments with a bulk size of 300–500 bp. Samples were centrifuged to pellet cell debris. The amount of chromatin isolated was quantified using nanodrop; an aliquot of this material was used as input for final quantification. Samples (0.5–1 mg of chromatin) were diluted with Triton buffer (100 mM Tris pH 8.6, 0.3% SDS, 1.7% Triton X-100

and 5 mM EDTA) to 1 ml and pre-cleared for 2 h with a mix of protein A and G (previously blocked with 5% BSA) at 4 °C. Antibody-coated beads were added: anti-NR5A2 (1 µg), anti-JUN (1 µg), anti-JUNB (1 µg), anti-FOS (5 µg), anti-JUND (2 µg), anti-H3K27ac (1 µg) and anti-H3K27me3 (1 µg). Non-related IgG was used as a control. After incubating for 3 h at 4 °C in a rotating platform, beads were successively washed with 1 ml of mixed micelle buffer (20 mM Tris pH 8.1, 150 mM NaCl, 5 mM EDTA, 5% w/v sucrose, 1% Triton X-100 and 0.2% SDS), buffer 500 (50 mM HEPES at pH 7.5, 0.1% w/v deoxycholic acid, 1% Triton X-100, 500 mM NaCl and 1 mM EDTA), LiCl detergent wash buffer (10 mM Tris at pH 8.0, 0.5% deoxycholic acid, 0.5% NP-40, 250 mM LiCl and 1 mM EDTA) and TE (pH 7.5), and then bound molecules were eluted by incubating overnight in elution buffer (containing 1% SDS and 100 mM NaHCO₃) at 65 °C, and treated with proteinase K solution (10 M EDTA, 40 mM Tris-HCl pH 6.5, 40 µg ml⁻¹ proteinase K). The eluted DNA was purified by phenol-chloroform extraction. After isolation, pelleted DNA was resuspended in 150 µl of nuclease-free water. Gene occupancy was then analysed by real-time PCR using 1 µl of the eluted DNA diluted in a final volume of 10 µl. The sequence of the primers used for ChIP-qPCR is provided in Supplementary Table 5.

Sequential ChIP. Chromatin from total pancreas was isolated as described above. In brief, after the first round of immunoprecipitation all beads were washed as described for the individual ChIP. Then, 10% of the beads were transferred to a new tube and de-crosslinked. The DNA was then extracted with phenol chloroform to check the efficiency of the first ChIP. For all steps involving immunoprecipitation, low protein-binding tubes were used (Eppendorf, 022431081). For sequential ChIP, the immune complexes in the remaining 90% of beads were eluted by incubating for 30 min at 37 °C in 90 µl of freshly prepared TE and 10 mM DTT, diluted to 2 ml with dilution buffer and incubated with anti-NR5A2 and anti-JUN antibodies overnight at 4 °C. Then, immune complexes were incubated with 40 µl of beads for 2–4 h at 4 °C, washed, transferred to a fresh tube and eluted as described for the individual ChIP.

NR5A2 and NR0B2 knock-down. NR5A2 expression was interfered using Mission shRNA lentiviral constructs purchased from Sigma-Aldrich (TRCN0000025966, targeting CCGGGCAGAAGACTACCTGTACTATCTCGAGATAGTACAGGTAGTCTTCTGCTTTTT (NR5A2 sh1) and TRCN0000025985, targeting CCGGCCACAACAGACTGAGAAATCTCGAGAA TTTCTCAGTCTGTTGTGGGTTTT (NR5A2 sh2)) previously tested for their efficiency. The knockdown efficiency was analysed by qRT-PCR and immunoblotting. NR0B2 expression was interfered using Mission shRNA lentiviral constructs purchased from Sigma-Aldrich (TRCN0000027118, targeting CCGGCGTCCGACTATTCTGTATGCACTCGAGTGCATACAGAATAGTCGG ACGTTTTT (NR0B2 sh1) and TRCN0000027130, targeting CCGGCA AGGAGTATGCGTACCTGAACCTCGAGTTCAGGTACGCATACTCCTTGT TTT (NR0B2 sh2)). Control cells were transformed using scrambled vector (shNT).

HEK293-FT cells (ATCC) were used to produce lentiviral particles. In brief, cells were allowed to reach 60% of confluence and transfected with 25 µg of shNT, sh1 or sh2 plasmids together with 30 µg of psPAX and 10 µg of pCMV-VSVG helper plasmids using CaCl₂ 2 M HBSS, as described earlier. After 12 h, the supernatant was collected and replaced with 5 ml of fresh medium. The supernatant was additionally collected 24 h and 48 h after transfection. The medium was filtered (0.45-µm pore) and added to 266-6 cells (at 50–60% of confluence). After three rounds of infection, the supernatant was removed and replaced with fresh medium. After one day of recovery, puromycin (2 µg ml⁻¹) (Sigma-Aldrich) was added. Two days later, the medium was replaced and cells were collected for protein and RNA analysis after 24 h.

NR0B2 lentiviral overexpression. The production of lentiviral particles and cellular infection were performed as described earlier. The medium from the transfectants was collected 12, 24 and 48 h after transfection. Subsequently, 266-6 cells (obtained from I. Rooman) were infected using polybrene (hexadimethrine

bromide, Sigma-Aldrich 107689) (5 µg ml⁻¹). After selection with puromycin, resistant 266-6 cells were collected for RNA and protein analysis.

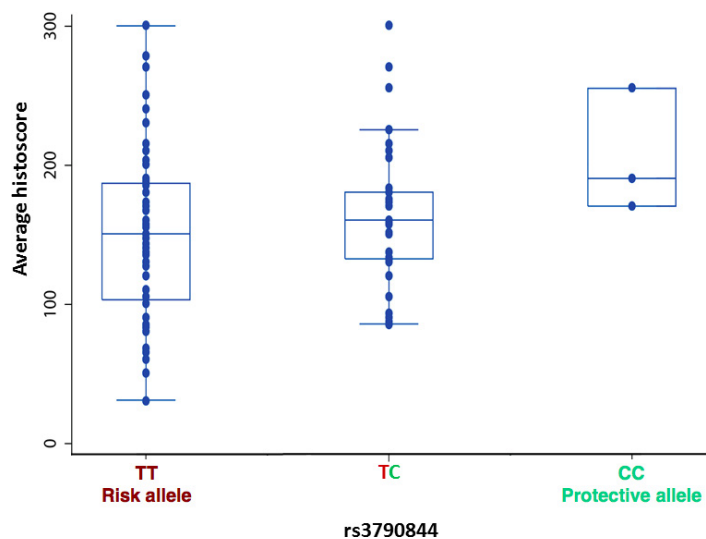
For combined NR5A2 knockdown and NR0B2 overexpression, cells were first incubated with control shRNA- or NR5A2-targeting lentiviruses. After puromycin selection, resistant 266-6 cells were allowed to recover in fresh medium and incubated with a medium containing lentiviral particles for empty vector or a medium containing lentiviral particles for NR0B2-Flag. Two rounds of infection were performed. After 24 h, the supernatant was removed and fresh medium was added. One day later, 266-6 cells were collected for protein and RNA analyses.

Cloning. NR5A2 cDNA was amplified and Flag-tagged by PCR using the following primers: GGGAATTCATGGACTACAAGGACGACGATGACAAGTCT GGCTAGTTTGG and GGGGAATTCCTTAGGCTCTTTTGGCATGCAGCA. The PCR product was ligated into the pJET vector and then sub-cloned into pLVX-puro. The human NR0B2 cDNA, tagged with a Flag epitope, was subcloned into the lentiviral vector pLVX-puro. The region encompassing –1960 to –655 of the mouse *Ccl8* promoter was amplified by PCR and subcloned in pGL3-basic vector (Promega). The sequence of the inserts was confirmed by enzymatic digestion and Sanger sequencing.

Luciferase reporter assays. HEK293T cells were transfected with plasmids pCDNA3-NR5A2-Flag and JUN-HA, or the corresponding empty plasmids, together with pRL-TK (Promega) constitutively expressing Renilla luciferase for normalization and transfection efficiency control. Plasmids containing the *Ccl8* promoter were included in all the experiments. The amount of transfected plasmids was maintained at a constant level. Transfections were performed using a standard CaCl₂ method and measurements were made in triplicate. After 36 h, cells were lysed in passive lysis buffer (Luciferase kit, Promega E2920) and reporter activity was determined using the Dual-Glo Luciferase Assay system (Promega), according to the manufacturer's instructions. Firefly and Renilla luciferase activities were measured using a luminometer.

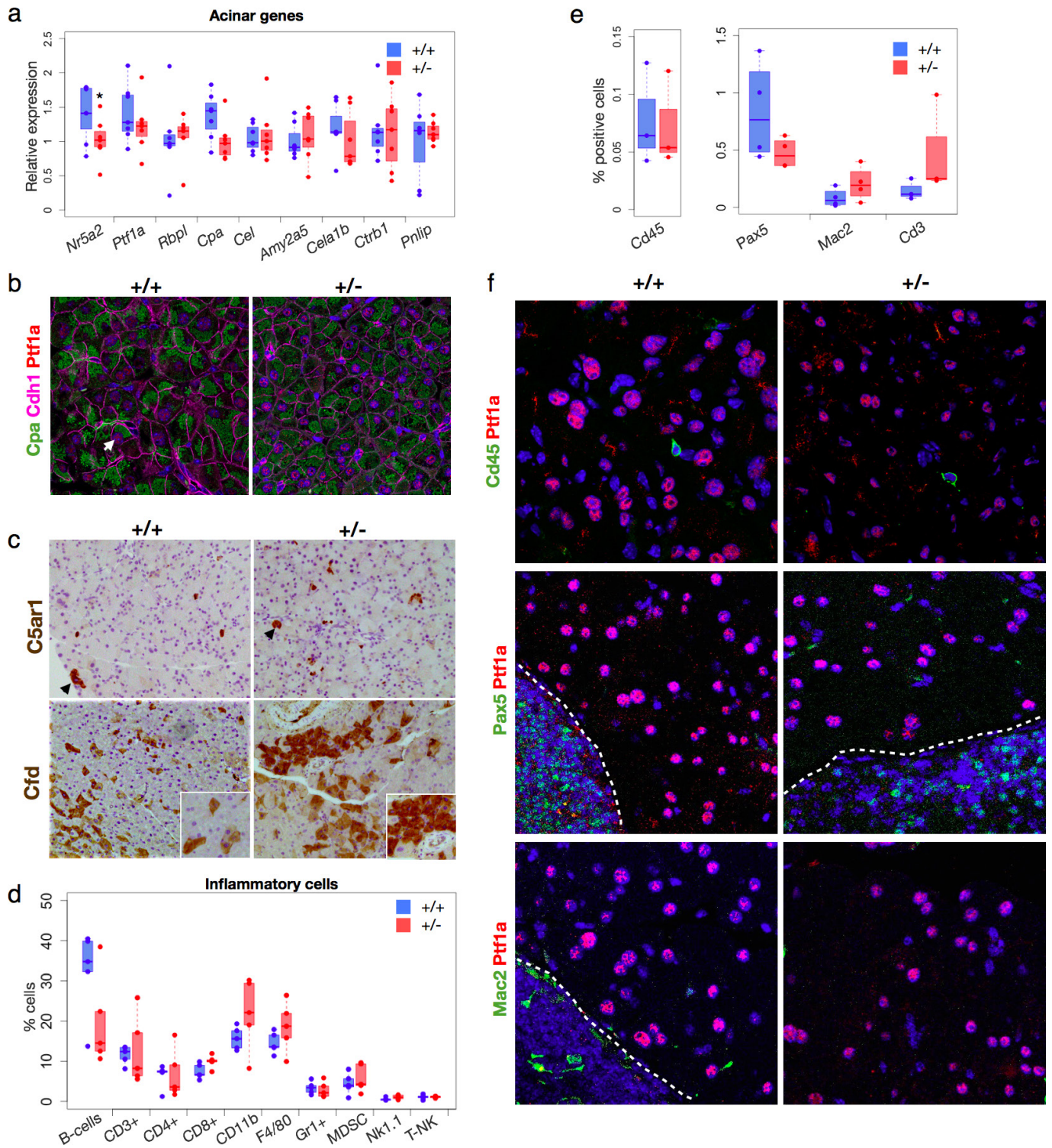
Other statistical analyses. Comparisons of quantitative data between groups was performed using one-sided Mann-Whitney *U* test in all cases for which there was a prior hypothesis, except for the data shown in Fig. 1g and Extended Data Fig. 5a. Box plots represent the median and first and third quartiles of the data; error bars are generated by R software and represent the highest and lowest data within 1.5× interquartile range. All statistical analyses were performed with Excel or R software. **Data availability.** Mouse pancreas RNA-seq data generated in this study have been deposited in GEO with accession number GSE84659. Source Data for Figs. 1–4 and Extended Data Figs 1–10 are provided with the online version of the paper. All other data are available from the corresponding author upon reasonable request.

- Botrugno, O. A. *et al.* Synergy between LRH-1 and β -catenin induces G1 cyclin-mediated cell proliferation. *Mol. Cell* **15**, 499–509 (2004).
- Behrens, A. *et al.* Impaired postnatal hepatocyte proliferation and liver regeneration in mice lacking *c-jun* in the liver. *EMBO J.* **21**, 1782–1790 (2002).
- Coste, A. *et al.* LRH-1-mediated glucocorticoid synthesis in enterocytes protects against inflammatory bowel disease. *Proc. Natl Acad. Sci. USA* **104**, 13098–13103 (2007).
- Clausen, B. E., Burkhardt, C., Reith, W., Renkawitz, R. & Förster, I. Conditional gene targeting in macrophages and granulocytes using LysMcre mice. *Transgenic Res.* **8**, 265–277 (1999).
- Kawaguchi, Y. *et al.* The role of the transcriptional regulator Ptf1a in converting intestinal to pancreatic progenitors. *Nat. Genet.* **32**, 128–134 (2002).
- Cendrowski, J. *et al.* Mnk1 is a novel acinar cell-specific kinase required for exocrine pancreatic secretion and response to pancreatitis in mice. *Gut* **64**, 937–947 (2015).
- Hoskins, J. W. *et al.* Transcriptome analysis of pancreatic cancer reveals a tumor suppressor function for HNF1A. *Carcinogenesis* **35**, 2670–2678 (2014).
- Li, B. & Dewey, C. N. RSEM: accurate transcript quantification from RNA-Seq data with or without a reference genome. *BMC Bioinformatics* **12**, 323 (2011).
- Wang, K. *et al.* MapSplice: accurate mapping of RNA-seq reads for splice junction discovery. *Nucleic Acids Res.* **38**, e178 (2010).



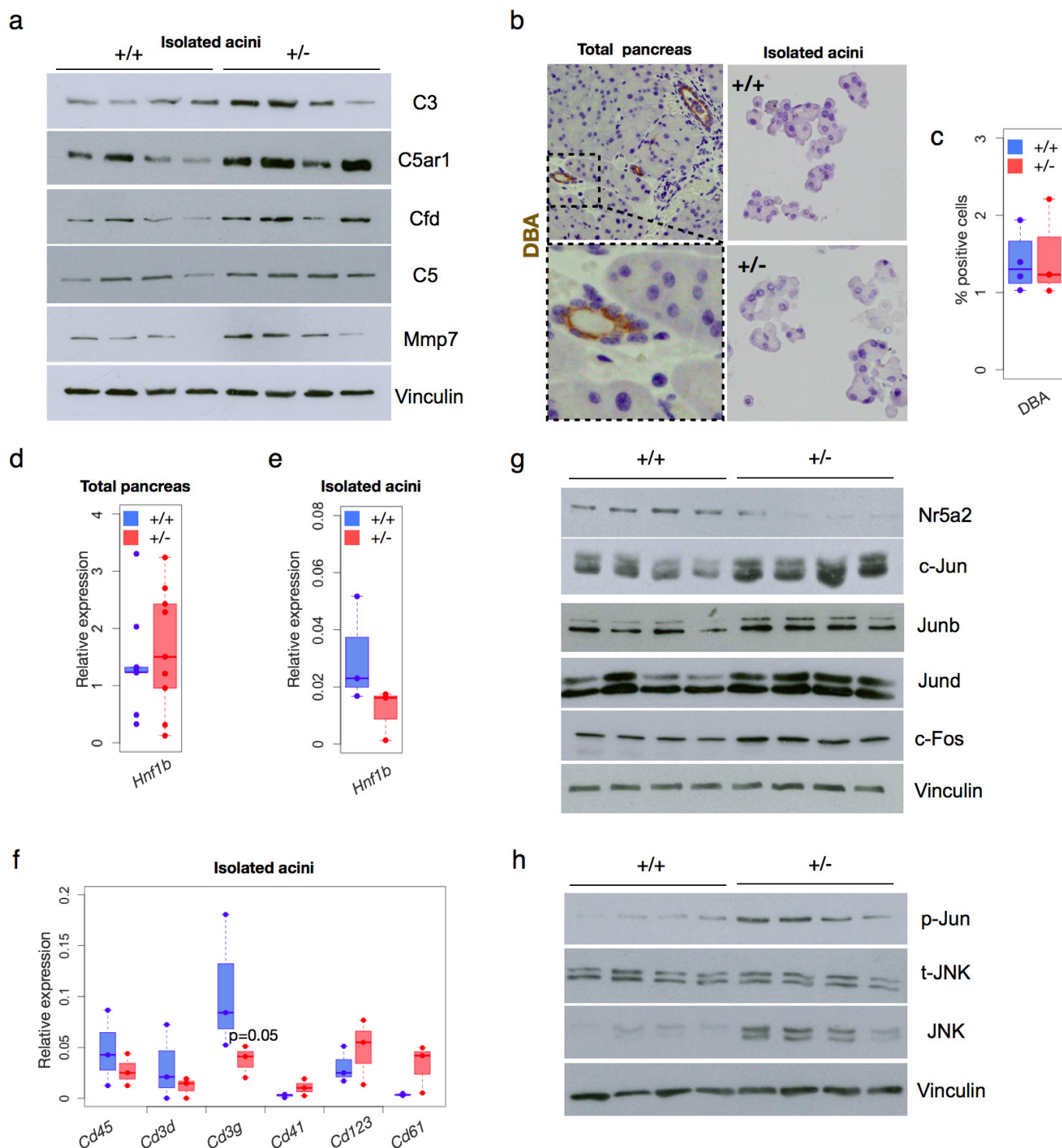
Extended Data Figure 1 | Protein eQTL analysis in human PDAC.

Pancreatic tumours ($n = 110$) from patients carrying the risk-increasing allele (T) at rs3790844 express lower levels of NR5A2 protein than those carrying the protective allele (C). NR5A2 expression was assessed using immunohistochemistry, and scored based on percentage of reactive cells and intensity of staining. The analysis was performed for mean histoscore ($P = 0.097$, $\beta = -18.0$; two-sided Wilcoxon test) and mean histoscore quantiles ($P = 0.028$, $\beta = -0.57$; two-sided Wilcoxon test).



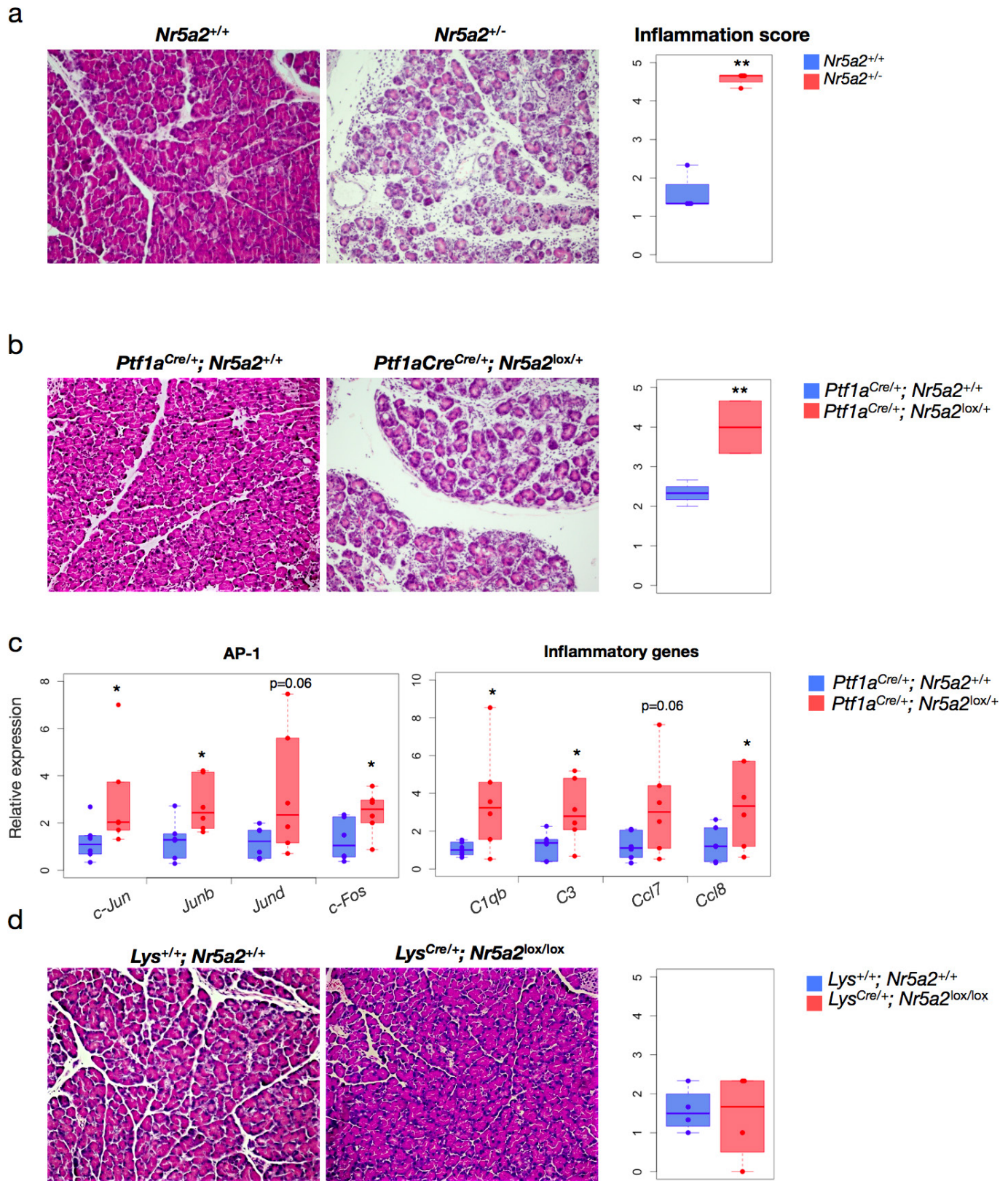
Extended Data Figure 2 | The pancreas of $Nr5a2^{+/-}$ mice is histologically normal but displays increased expression of inflammatory genes. **a**, qRT-PCR analysis of the expression of transcripts coding for acinar-related genes in wild-type and $Nr5a2^{+/-}$ mice ($n = 7$ per group). Data were obtained from a series of mice that was independent of the series used for RNA-seq. **b**, Immunofluorescence analysis of PTF1a, CDH1 and CPA in the pancreas of wild-type and $Nr5a2^{+/-}$ mice ($n = 3$ per group). Arrow, acinus. **c**, Immunohistochemical analysis of expression of C5AR1 and CFD in the pancreas of wild-type and $Nr5a2^{+/-}$ mice shows patchy expression in acinar cells (arrows) ($n = 5$ per group). **d**, Percentage

of inflammatory cell subtypes (from total cells) in wild-type and $Nr5a2^{+/-}$ pancreases ($n \geq 4$ per group) analysed by flow cytometry (two different experiments). **e**, **f**, Quantification of periacinar $Cd45^{+}$ cells in the pancreas of wild-type and $Nr5a2^{+/-}$ mice using immunofluorescence on frozen sections. Broken line delineates a pancreatic lymph node, used as a control. Two independent assessments were performed. **e**, Quantification of cells expressing PAX5, MAC2 and CD3 in the pancreas of wild-type and $Nr5a2^{+/-}$ mice using immunofluorescence ($n \geq 3$ per group). In **a**, **d** and **e**, one-sided Mann-Whitney U test; * $P < 0.05$, ** $P < 0.01$.



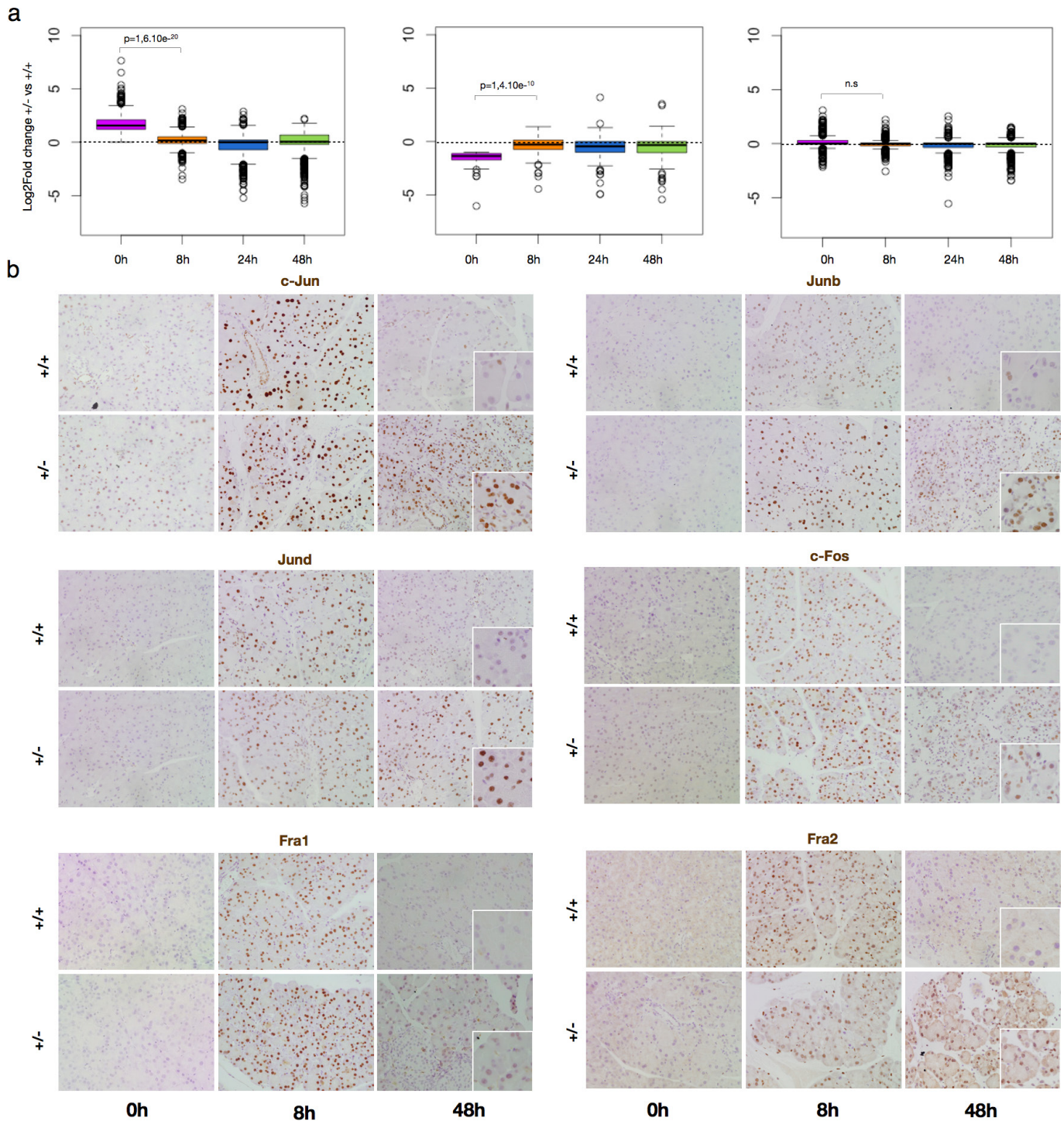
Extended Data Figure 3 | The upregulation of inflammatory markers, AP-1 components, p-JUN and p-JNK in *Nr5a2*^{+/-} pancreases is epithelial-cell-autonomous, as shown by the analysis of isolated primary acinar cells. a, Expression of inflammatory proteins in primary acinar cells from wild-type and *Nr5a2*^{+/-} mice shown using western blotting ($n = 4$ per group). **b–f**, Primary acinar cell fractions from wild-type and *Nr5a2*^{+/-} mice largely depleted of DBA⁺ ductal cells (b, c),

show reduced expression of the ductal cell marker HNF1 β (d, e) and inflammatory cell markers (f) compared to total pancreas ($n = 4$ per group). Inset in b, DBA-labelled duct. Two independent experiments were performed. **g, h**, Expression of AP-1 components and JNK in primary acinar cells from wild type and *Nr5a2*^{+/-} mice using western blotting. NR5A2 is expressed at reduced levels in *Nr5a2*^{+/-} pancreases ($n = 4$ group). In c–f, one-sided Mann–Whitney U test; * $P < 0.05$, ** $P < 0.01$.



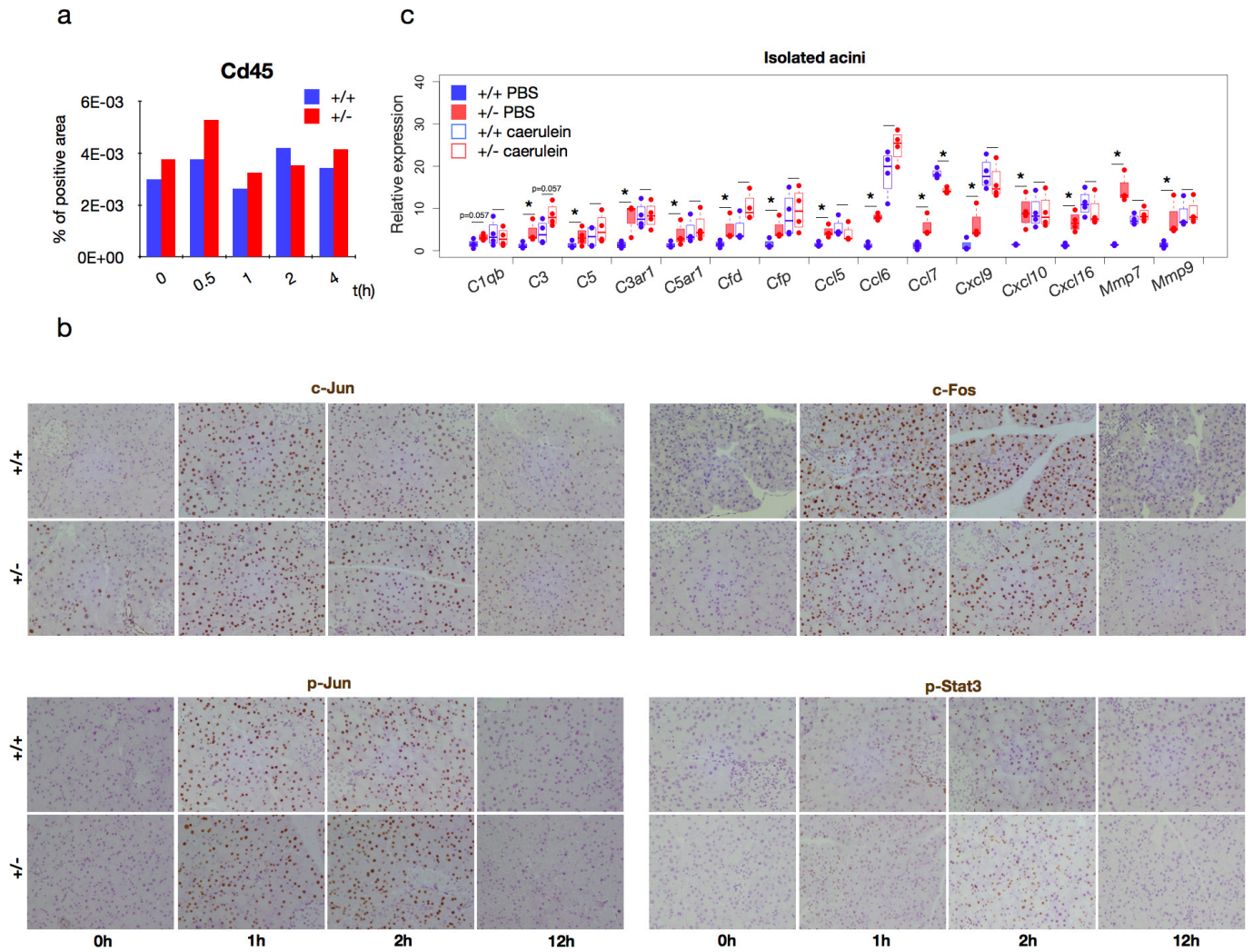
Extended Data Figure 4 | The defective pancreatic response to damage is epithelial-cell-autonomous. **a**, Constitutive *Nr5a2*^{+/-} mice display more severe pancreatitis upon administration of seven doses of caerulein (given once per hour). **b**, **d**, This severe phenotype is recapitulated at 48 h in mice harbouring a heterozygous deletion of *Nr5a2* in pancreatic epithelial cells (**b**) but not in mice in which both alleles of *Nr5a2* are inactivated in myeloid cells by Cre activation from the lysozyme endogenous locus (*Lys*) (**d**). This experiment was performed once for

the conditional mice; for *Nr5a2*^{+/-} mice, more than four independent experiments were performed. Representative histological images are shown. Semi-quantitative inflammation scores corresponding to the experiments are shown in **a-d** ($n \geq 4$ per group). **c**, qRT-PCR analysis of the expression of transcripts coding for AP-1 and inflammatory genes in control and *Ptf1a*^{Cre}; *Nr5a2*^{lox/+} mice ($n = 6$ per group). In **a-d**, one-sided Mann-Whitney *U* test; * $P < 0.05$, ** $P < 0.01$.



Extended Data Figure 5 | *Nr5a2* haploinsufficiency causes a basal pre-inflammatory state similar to that associated with the early stages of pancreatitis. a, Comparative expression (wild-type versus *Nr5a2*^{+/-} mice) of the upregulated (left), downregulated (middle) or control (right) genes over time, after induction of pancreatitis. RNA-seq analysis was performed

once. One-sided Student's *t*-test. **b,** Immunohistochemical analysis shows persistent overexpression of AP-1 components during the recovery period after induction of acute pancreatitis (one dose per hour for seven hours). Representative results of one of five pancreases analysed are shown.



Extended Data Figure 6 | A single dose of caerulein does not cause inflammation but does induce an upregulation of AP-1 and p-JUN that precedes STAT3 phosphorylation both in wild-type and *Nr5a2*^{+/-} mice. **a**, Quantification of infiltration by Cd45⁺ cells in the pancreas of wild-type and *Nr5a2*^{+/-} mice after administration of one dose of caerulein ($n = 1$). **b**, Immunohistochemical analysis of expression of JUN, FOS, p-JUN and phospho-STAT3 (p-STAT3) in wild-type and *Nr5a2*^{+/-} mice at various

time points after caerulein administration ($n = 4$ per group). **c**, qRT-PCR analysis of expression of a panel of inflammatory genes in isolated acini treated with PBS or caerulein (100 pM). Data are shown relative to values of wild-type acini incubated with PBS ($n = 4$ per group). Two independent experiments were performed. In **c**, one-sided Mann-Whitney U test; * $P < 0.05$, ** $P < 0.01$.

a

C1qb promoter (-1581;-655)

GGTCCTGATGTATAGACCCTGTCTGCTCCAAGTCTGTCCCCTTTCATATACATAACTGTGTCT
 GAGGGCCCTGGACTTTGAAGTTCTCCCTCGTTTCAACCAACAGCCCCAGGAAACAGGCTCTA
 CCATCTCTGATGTAGACCTGAGAGAAGCCCACTTAAGAACATGCTTTGGCCATATGACTGGAAA
 CTGGGGTTTCAAACTAGGGAGTTCAGATTTTCTACTGGCAATTACTCAAGGAATCAGAGACTCA
 GCCTAGGACCCTCAGAGGGACCCGAGGCTGGTGATCACGATGCACACCTGTAATCCAGTACG
 TGGGAGACAGAGAGACCACGGGATTTAAGTCTGAGGCCAACCTGGGATAAAAAGAGTGAGAC
 CCTGCCCTCAAGCTAAGTAAGTACAGAGCCGGTTCCCTGGGCACATGGCCCTCAGCTCCTCCAT
 CTCTTTTGAACCTGGCTGAGTCACTCTCTTTTCTCTTGTCCCTCTGGTATTGGGGTACACCTG
 GCTGTACTTACACACAGTACAGCAGCAGCAGCTAGACCCTGGCCCCAGAGCTCTCTGGCTTCT
 GGGTCTGCTCTGGAGCATGGGTTCTAAAATTCAGTATTTTCTGTGACATTTACCACAGAAACAT
 TTAATGTTAACTCCAGCCTCCCATAAAGGGATGCCCTCAAAGGACAGGACTCTTGTACCCCT
 TAAGCCCTTCTCCCTAGACTATAGTCTCATAGTATTTGTCCCCCTCCAACAAAGTCCGGTTGG
 ATGATAACTCATGGCTCAGACCTCATTCCCTGAGTGTAAAGTGAGGGACAGGGTGGGCACAG
 TGACCTCAAAGCCCTCCGCAGCTCTGTCTGTGTCATTCCATAGGGAGCAGTCCCTTCTCTG
 TGGCTGTTATGTCAAGGGCTCAAGC

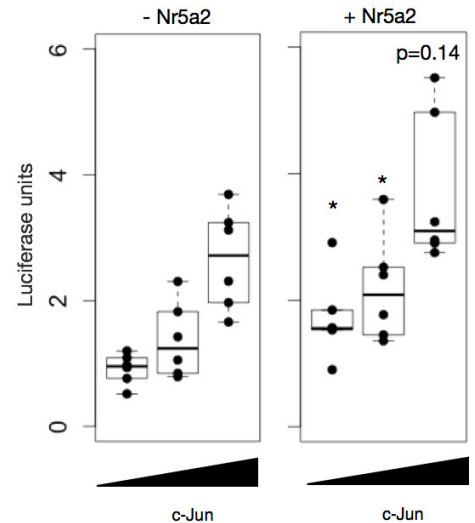
Ccl7 promoter (-590;+364)

AAAGAATGCTTTGGATGGCCCTCAACTTCAGCCGCTACCTACAACCAAGTACTGGCCAGCTG
 ATGCCAGTCAACTTTCCCAATAAAGAGCTGTTTTGTTTTAGTAAATATAATAGACACAG
 GGTTTGGAAATGTTTTATGATTTTTGTTGTCTGTTTCAAAACATCTTTTCTCTGTGGTTTGA
 AATAGCAGGACTTTTTCATCTCAAGTGCATTTTTAAATTCAGTCAAAAATTTAGTGCCTGTTTCTAG
 ACTCCAAAGCTCCTTGGGATGTTGCTCGAAGGGGAAATAGGAATCCCTTGACTCTGCCATCTCT
 GCTTCCCTCCTCACTTCTCAAAAAAAGAGGCTGTTTTGTTTTAGTAAATATAATAGACACAG
 GTAAGTGCAGCTGGTTGGAAATAGCCAGAGTTCACAGTACAGTGTTTTATCTGGACAAGTCA
 CCTCATTTTCCATTCCTGCTGTTAAATGGAATAGGCCAGCCCTCACATTACACTCTCCTGTGATC
 ATTCCAAAAGAAGATCCCTCCCTATCGGCTGCCTATAAAAGAGGAGGACAGCTGCCAGAAGAG
 CAGAGAAGCAAGGCCACACAGAGTCTGCCAGCTCTCACTGAAGCCAGCTCTCTCACTCTCT
 TCTCCACCATGAGGATCTCTGCCAGCTTCTGTGCCTGCTGCTCATAGCCGCTGCTTTCAGCAT
 CCAAGTGTGGCCCAACCAAGGTGAGACTCACCTGCCTCTGTTTCCAGAGCATGCTGTCCCT
 TTCTCTGGGACATTTTCATAGAAAAATACAGAACAAGGTTTACCCATAGTCTCACATTTGCTGGCTT
 GCCAAAGTAGGACAATTAAGAAAGGACAAGATACTTATAGTCCAATGATAATCTAGAACTTG
 AACCTGATCCCTTAGGACTCAATTTGTGGAACAAGATAG

Ccl8 promoter (-1960;-655)

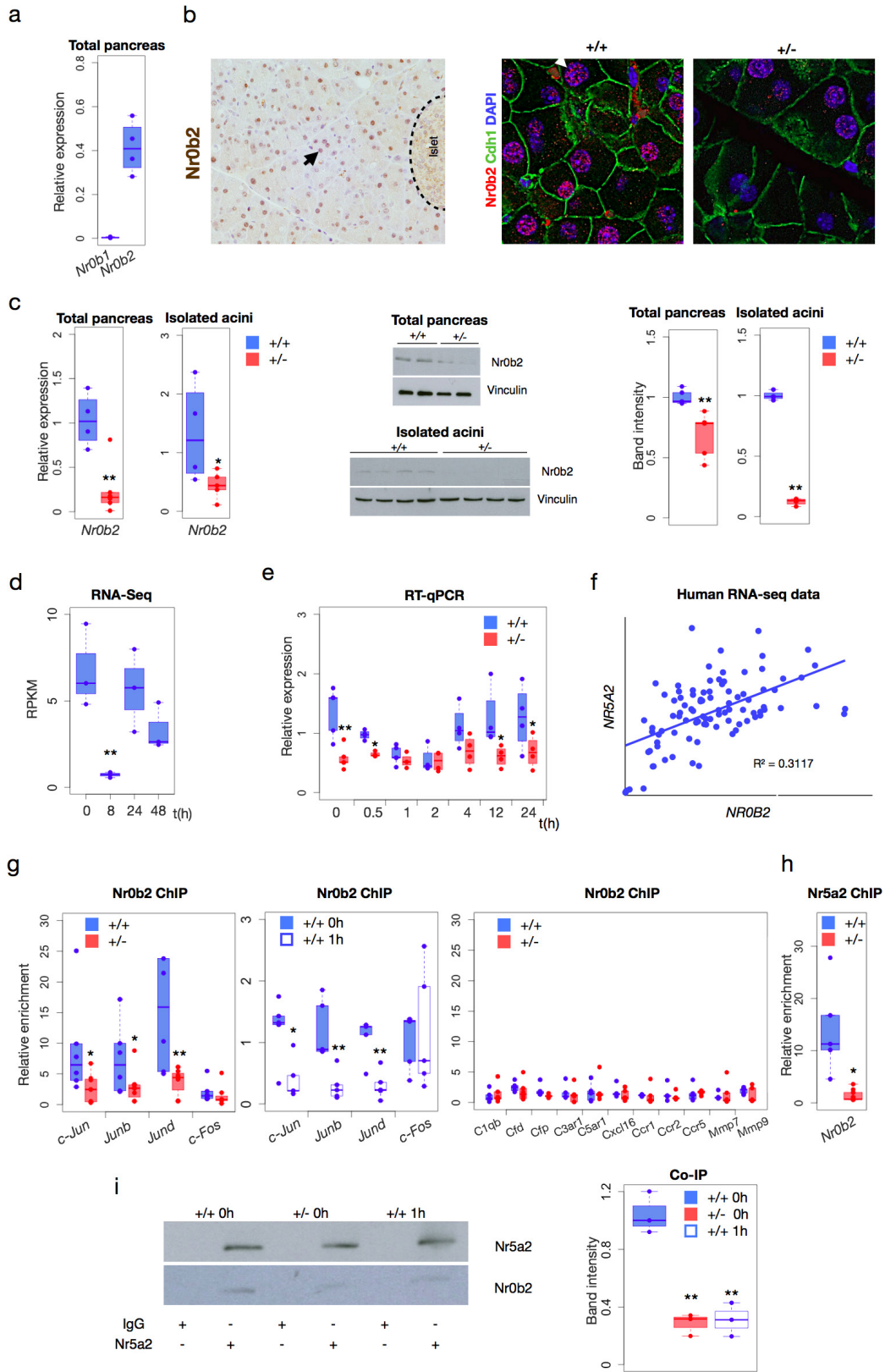
GGAGAACCCTCCACACTGAGCTCTTCCAAATTTACTTTGTCCGGAAGAACCCTCCACACTGAT
 TTCCATAGTAAAAAATTCGTGATGAGTGCCAGAGATGTTGTGTCAGACT
 TCTATTTGGGCTCCTATTTTATACATCAATCAGTGTCTGGTTTTGTCTACTAATTAAGATAT
 AAACCTTAGATTCATTAATACTAAAGGTGATAAACACTTTGGTTCAAACATTTACCTCAAACCTG
 TACCAACTCCTGCTGCCCTTGTGGCCTGCAGAAATGCTGACTCGTGTCTTCTTCACTACGACG
 ACAGTTGGGTATTGTAAGTGCCTAAGCTTGAGTCCAACAACATTTCCAAATTTCTCCGTTTCAATGTT
 TCTTAAATCATTTCTTTTATGATATTTGAAAACCTGTCTTAGGCATTTGAAATTTCTTTTAATA
 TTTTCTAAGTGACAAACAGTGTGATAAATCATGCTGCAGGGAAGGTTCAAATTAAGTAAAGCCATGC
 CCTTAGTCCATCATGCTTTCTTATGCTGTTTGCCTTCTCACACTTCAAACCTTGTCTGAAACAAG
 TCTTCATTCGAAAAAGACTCTGTAGACACAGGAAAAATCACTTGGATTAAGGAGTGTGATG
 ACTCATGACATACTGAGGAGTTTGGCCCTTCTTGTCTTTGGTTTCTTTGGGTTGTTTTGTTGTTG
 TGGGGTTTTTTGTTGTTGTTGTTGTTGTTGTTGTTGTTGTTGTTGTTGTTGTTGTTGTTGTTGTTG
 GTTATACTTTAGATATAATGTACTACTGTGTGTTGCAATTTAAATGTTGTAGCTGACAGAGGTCAAAA
 CCCAGAAAAATCATAAATATTAGCCATTAGCTCATGGGCTTAATAGATTGGATATAATTACAGAGA
 TTAAATCTGAGTGGCTTTACTAATATATCCCTCACTTGAGGATGTTCTTCTGCTACTAGTCA
 GAATCTTTGCTTACACTGACGAGGAATGAGACTGAGCATAACACTATTTGGCCCTCCAAACACATT
 GAACAGGATGCTTGGCCAACAGAGTATTGTGATTGAAGTCCCAGACAAAAGTCATACATACATT
 AAGGATTTGCAAGAAAACAGCTCTGTGATGTAGAGAGCTATGCTCTGCAGGATGCCACCCGC
 TGCAGGATCCCTGCCCTCCAGAATCCACACGTTGGTCCCAAGTCTCCAGGACTTTTCAGGCTA
 GGCCAGACATAGTAGAAAACCTGTTATTACAGCATTTCAGACTGATATGGGAGAATTATACA
 CAAGGACGGCCCTGGGACAAGTAAATTTGGAAGAGC

b



Extended Data Figure 7 | NR5A2 cooperates with AP-1 to regulate inflammatory gene expression. a, Analysis of putative NR5A2 and AP-1 binding sites in the proximal promoter of *C1qb*, *Ccl7* and *Ccl8* using the JASPAR algorithm ([http://jaspar.genereg.net/search?q=&collection=](http://jaspar.genereg.net/search?q=&collection=CORE&tax_group=vertebrates) CORE&tax_group=vertebrates). Sequence matrices for NR5A2, FOS:JUN, FOS, JUN, JUN (var.2), FOSL1, FOSL2 and BATF:JUN were computed. Motifs with a score of greater than 7.5 for NR5A2 (blue) and AP-1 (orange) are highlighted. Additionally, a manual search for the NR5A2

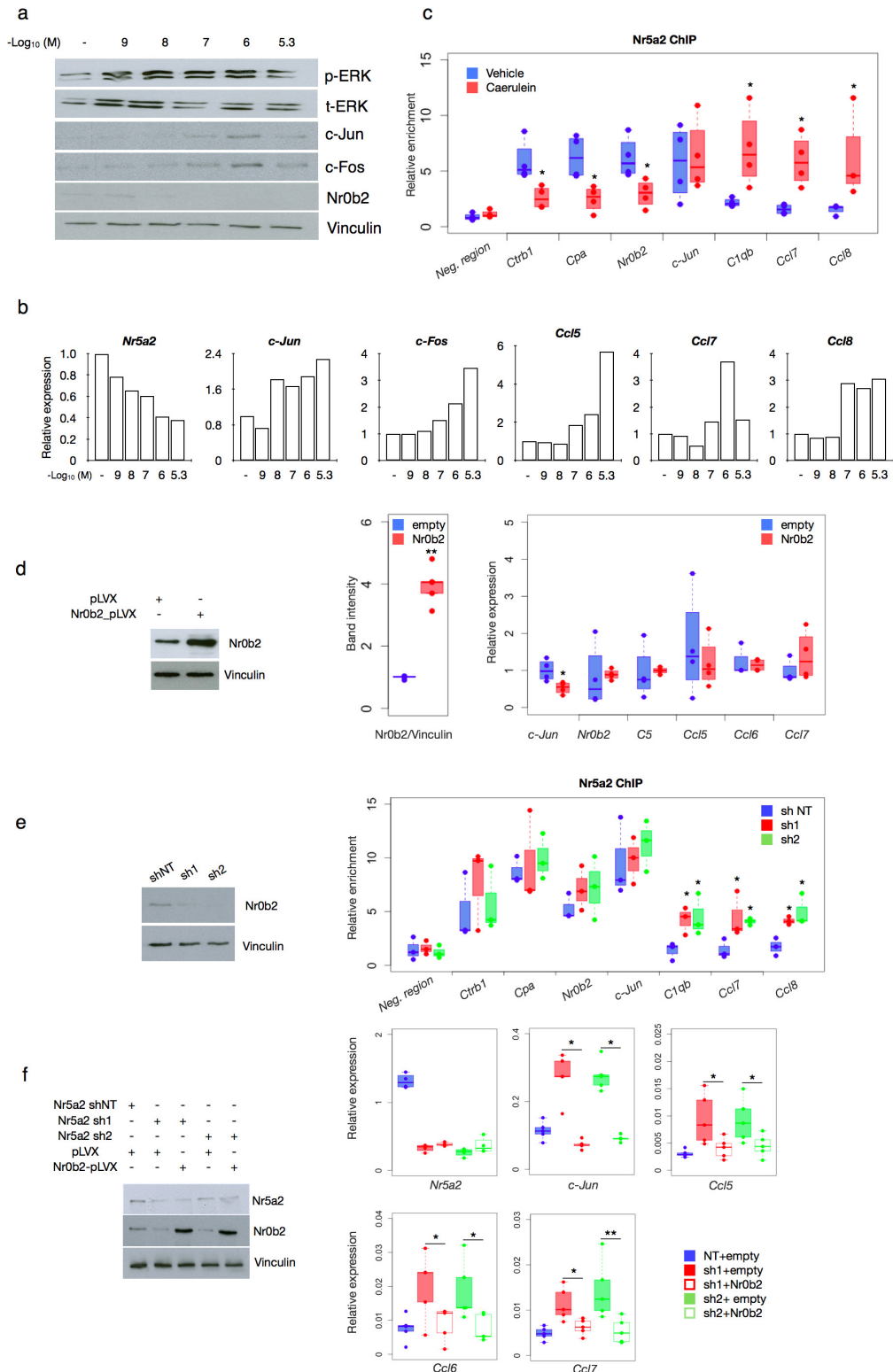
binding motif CAAGNCA was performed. Purple, genomic regions amplified in the sequential ChIP-qPCR experiments shown in Fig. 3f. The sequences of the 400 nucleotides upstream and downstream of each amplicon are also shown. b, *Ccl8* luciferase promoter-reporter activity (-1960 to -655) using HEK293 cells and increasing concentrations of JUN-coding plasmid in the absence (left) or presence (right) of NR5A2. Data shown corresponds to the mean of six independent experiments. In b, one-sided Mann-Whitney *U* test; **P* < 0.05, ***P* < 0.01.



Extended Data Figure 8 | See next page for caption.

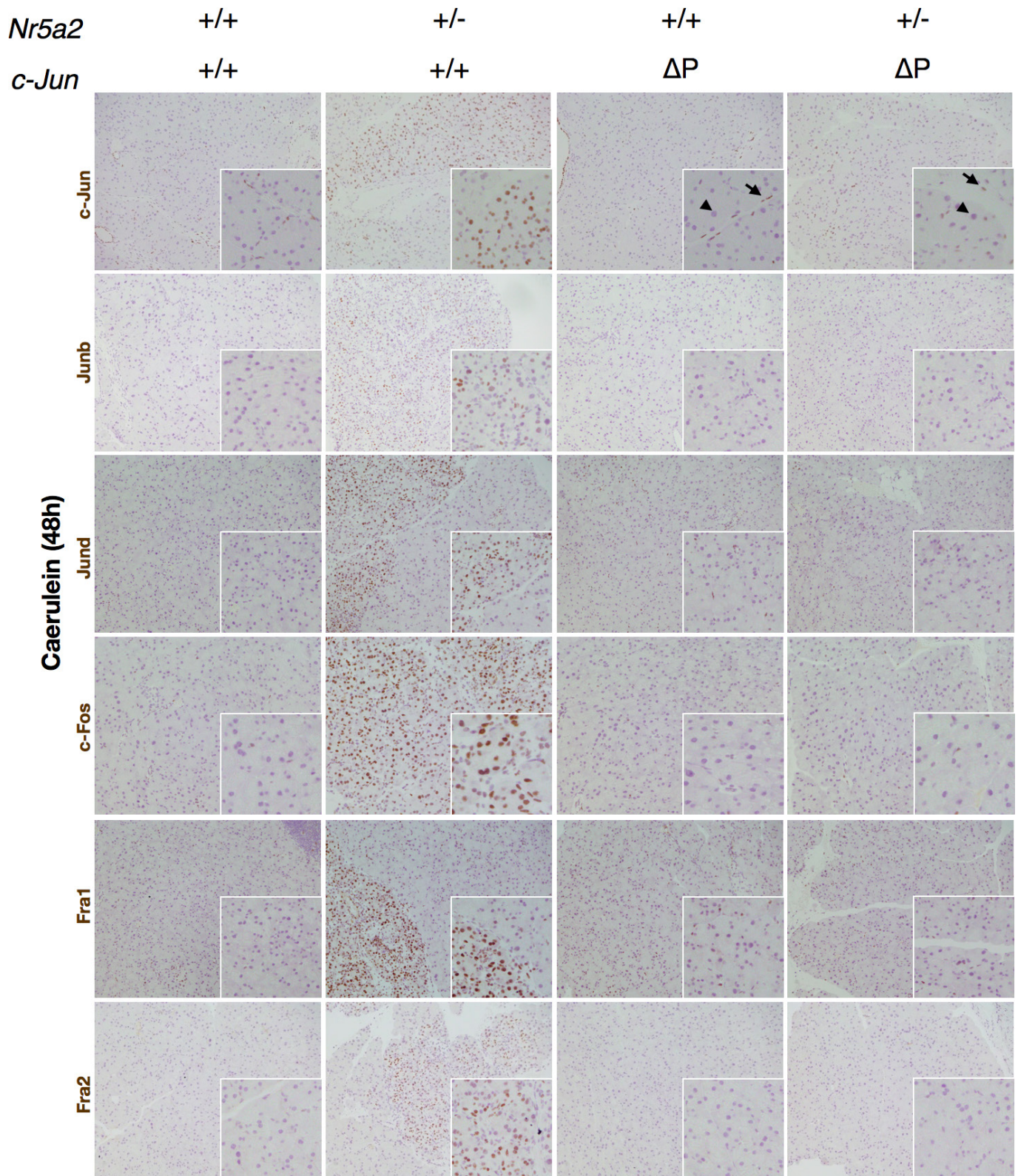
Extended Data Figure 8 | NR5A2 regulates AP-1 expression, in part through the modulation of NR0B2 and its recruitment to AP-1 gene promoters. **a**, Expression of *Nr0b1* and *Nr0b2* transcripts in total pancreas and isolated acini of wild-type and *Nr5a2*^{+/-} mice ($n = 4$ per group). Arrow, acinus; broken line delineates an islet. **b**, Immunohistochemical and double immunofluorescence analysis showing acinar distribution of NR0B2 in wild-type pancreas, and reduced expression in *Nr5a2*^{+/-} pancreases. Acinar cells are delineated with anti-CDH1 antibodies ($n = 5$ per group). **c**, Reduced expression of *Nr0b2* mRNA and corresponding protein in total pancreas and isolated acini of wild-type and *Nr5a2*^{+/-} mice. Densitometric quantification of NR0B2 expression relative to vinculin ($n \geq 4$ per group). **d, e**, Expression of *Nr0b2* mRNA in wild-type mice on induction of mild acute pancreatitis (**d**) ($n = 3$ per group) or on administration of a single dose of caerulein (**e**) ($n \geq 3$ per group). **f**, Correlation of *NR5A2* and *NR0B2* mRNA expression in normal human pancreas using RNA-seq. **g**, ChIP-qPCR analysis of the

occupancy by NR0B2 at the AP-1 (left) and inflammatory gene promoters (right panel) in wild-type and *Nr5a2*^{+/-} mice. In the left and right panels, data are shown relative to control IgG and an unrelated genomic region ($n = 3$ per group). ChIP-qPCR analysis of NR0B2 on the promoter of AP-1 genes shows reduced occupancy in wild-type mice 1 h after administration of one dose of caerulein. Results in the middle panel are normalized to enrichment in wild-type mice ($n \geq 6$ per group). **h**, ChIP-qPCR analysis of the occupancy of the *Nr0b2* promoter by NR5A2 in wild-type and *Nr5a2*^{+/-} mice. Data are shown relative to control IgG and an unrelated genomic region ($n \geq 5$ per group). **i**, Co-immunoprecipitation of NR5A2 and NR0B2 in wild-type and *Nr5a2*^{+/-} pancreases under basal conditions or 1 h after administration of a single dose of caerulein. Densitometric quantification of NR0B2 bands (right) ($n = 3$ per group). At least two independent experiments were performed. In **a–i**, one-sided Mann–Whitney U test; * $P < 0.05$, ** $P < 0.01$.



Extended Data Figure 9 | NR0B2 has an important role in the dynamic regulation of inflammatory genes by NR5A2. a–c, Validation of 266-6 cells as a model for mechanistic studies. a, Dose-dependent effects of caerulein on ERK activation, AP-1 expression and NR0B2 expression shown using western blotting. b, qRT-PCR analysis showing caerulein-induced changes in expression of *Nr5a2*, *AP-1* and inflammatory genes. c, ChIP-qPCR analysis showing changes in NR5A2 occupancy of the promoters of acinar (*Ctrlb1*, *Cpa* and *Nr0b2*), *Jun* and inflammatory genes (*C1qb*, *Ccl7* and *Ccl8*) 30 min after treatment with caerulein (4 independent experiments) These findings largely recapitulate the observations made in the mouse pancreas. d, Forced overexpression of

NR0B2 leads to reduced expression of *Jun* mRNA but does not affect expression of inflammatory genes (four independent experiments). e, Effects of NR0B2 knockdown on NR5A2 binding to the promoter of acinar, *Jun* and inflammatory genes (three independent experiments). f, Combined NR5A2 knockdown and NR0B2 overexpression showing that higher levels of NR0B2 are associated with reduced expression of inflammatory gene transcripts, a situation that mimics normal pancreas under basal conditions in wild-type mice (four independent experiments). At least two independent experiments were performed. In c–f, one-sided Mann-Whitney *U* test; **P* < 0.05, ***P* < 0.01.



Extended Data Figure 10 | JUN is required for the overactivation of AP-1 that is observed in *Nr5a2*^{+/-} mice during caerulein-mediated pancreatitis. Immunohistochemical analysis of the expression of JUN, JUNB, JUND, FOS, FOSL1 and FOSL2 in the pancreas of control

(*Nr5a2*^{+/+}, *Nr5a2*^{+/-} and *Nr5a2*^{+/+};*Jun*ΔP) and *Nr5a2*^{+/-};*Jun*ΔP mice 48 h after the initiation of pancreatitis (*n* = 4 per group). One experiment was performed. Arrowhead, acinus; arrow, mesothelial cell.

Life Sciences Reporting Summary

Nature Research wishes to improve the reproducibility of the work that we publish. This form is intended for publication with all accepted life science papers and provides structure for consistency and transparency in reporting. Every life science submission will use this form; some list items might not apply to an individual manuscript, but all fields must be completed for clarity.

For further information on the points included in this form, see [Reporting Life Sciences Research](#). For further information on Nature Research policies, including our [data availability policy](#), see [Authors & Referees](#) and the [Editorial Policy Checklist](#).

▶ Experimental design

1. Sample size

Describe how sample size was determined.

No previous sample size calculation was used. The number of mice used was based on the previous experience of the laboratory in using these assays and mouse strains. In selected cases, a pilot experiment was performed to decide the final number of mice to be used. For selected experiments (i.e. RNA-Seq) a "feasible" number of mice was used that was estimated to provide sufficient statistical power.

2. Data exclusions

Describe any data exclusions.

No data were excluded from the analysis except for two mice used for the flow cytometry analysis for which the cell viability was low and, therefore, inappropriate for analysis.

3. Replication

Describe whether the experimental findings were reliably reproduced.

In all major experiments, at least two and generally 3 experiments were performed.

4. Randomization

Describe how samples/organisms/participants were allocated into experimental groups.

Samples were allocated to experimental group (a randomization method was not used) without any previous selection. Stated in the text.

5. Blinding

Describe whether the investigators were blinded to group allocation during data collection and/or analysis.

Samples were coded. Experiments were performed and then data were decoded. The code was unknown to the investigator at the time of analysis.

Note: all studies involving animals and/or human research participants must disclose whether blinding and randomization were used.

6. Statistical parameters

For all figures and tables that use statistical methods, confirm that the following items are present in relevant figure legends (or in the Methods section if additional space is needed).

n/a Confirmed

- The exact sample size (n) for each experimental group/condition, given as a discrete number and unit of measurement (animals, litters, cultures, etc.)
- A description of how samples were collected, noting whether measurements were taken from distinct samples or whether the same sample was measured repeatedly
- A statement indicating how many times each experiment was replicated
- The statistical test(s) used and whether they are one- or two-sided (note: only common tests should be described solely by name; more complex techniques should be described in the Methods section)
- A description of any assumptions or corrections, such as an adjustment for multiple comparisons
- The test results (e.g. P values) given as exact values whenever possible and with confidence intervals noted
- A clear description of statistics including central tendency (e.g. median, mean) and variation (e.g. standard deviation, interquartile range)
- Clearly defined error bars

See the web collection on [statistics for biologists](#) for further resources and guidance.

► Software

Policy information about [availability of computer code](#)

7. Software

Describe the software used to analyze the data in this study.

- Immunohistochemistry quantification - AxioVision 4.6 software package, Zeiss
 - Flow cytometry analysis - FlowJo, LLC.
 - RNA-Seq analysis - Illumina Real Time Analysis software (RTA1.13); Fastqc (v0.9.4, Babraham Bioinformatics; Cufflinks (version 2.0.2); (MapSplice) RSEM version 1.2.14;
 - ChIP-Seq analysis: fastqc (v0.9.4, Babraham Bioinformatics); Burrows-Wheeler Aligner (bwa,v0.5.9-r16); Macs14 (v1.4.1 20110622); PeakAnalyzer 1.4

For manuscripts utilizing custom algorithms or software that are central to the paper but not yet described in the published literature, software must be made available to editors and reviewers upon request. We strongly encourage code deposition in a community repository (e.g. GitHub). *Nature Methods* [guidance for providing algorithms and software for publication](#) provides further information on this topic.

► Materials and reagents

Policy information about [availability of materials](#)

8. Materials availability

Indicate whether there are restrictions on availability of unique materials or if these materials are only available for distribution by a for-profit company.

There are no restrictions on the availability of our materials or data.

9. Antibodies

Describe the antibodies used and how they were validated for use in the system under study (i.e. assay and species).

A list with all antibodies used and antibody source and concentration is provided. Validation was performed following variable strategies: cellular distribution, size of bands in western blotting experiments, for critical antibodies knockout cells/tissues were used for validation. Crucial antibodies for the study were extensively validated based on previous work of the participating laboratories (i.e. AP-1 components, NR5A2, NROB2).

LIST OF ANTIBODIES USED

c-Fos. Cell Signalling CST, 9F6. 0.1 µg/mL (IHC). 0.1 µg/mL (WB).
 c-Fos. Santa Cruz, SC-52. 4 µg/mL (IHC). 0.1 µg/mL (WB). 2 µg/ChIP.
 c-Jun. Cell Signalling, CST 60A8. 0.5 µg/mL-0.25 µg/mL (IHC and IF). 0.05-0.1 µg/mL (WB). 2 µg/ChIP.
 C5ar1. Abcam, ab59390. 2.5 µg/mL (IHC). 1 µg/mL (WB).
 Cd45. Novus Biologicals, NB110-93609. 0.8 µg/mL (IHC).
 Cdh1. BD transduction, C20 820. 0.25-0.35 µg/mL (IHC,IF).
 Complement C5. Hycult Biotech, BB5.1. 1 µg/mL (IHC). 0.2 µg/mL (WB).
 Complement Factor D. Kindly provided by Minuro Takahashi, Japan. 1/200-1/400 (IHC). 1/1000 (WB).
 Cpa. RnD Systems, AF2765. 1 µg/mL (IF).
 Erk. CST, #9102. 0.1 µg/mL (WB).
 Flag-tag. Sigma, M2. 0.1 µg/mL (WB).
 Fos1 (Fra1). Santa Cruz, N-16. 1 µg/mL (IHC). 2 µg/ChIP.
 Fos2 (Fra2). Monoclonal Antibody Unit, CNIO. 1/200-1/400 (IHC and IF). 1/1000 (WB).
 H3K27ac. Abcam, 4729. 0.5 µg/mL (IHC). 0.05 µg/mL (WB). 1 µg/ChIP.
 H3K4me3. Millipore, 07-449. 0.5 µg/mL (IHC). 0.05 µg/mL (WB). 1 µg/ChIP.
 HA-tag. Sigma, F3165. 0.1 µg/mL (WB).
 Jnk. Cell Signalling, CST 9252. 0.1 µg/mL (WB).
 Junb. Cell Signalling, CST 37F9. 0.5-1 µg/mL (IHC). 0.1 µg/mL (WB). 3 µg/ChIP.
 JunD. Pfarr et al., 1994. 1/1000 (WB).
 Jund. RD Biosystems, AF5526. 2-5 µg/mL (IHC). 0.5 µg/mL (WB). 3 µg/ChIP
 Laminb. Santa Cruz, M-20. 0.25 µg/mL (WB).
 NroB2. Santa Cruz, H-160. 1.67-4 µg/mL (IHC,IF). 0.4 µg/mL (WB). 2 µg/ChIP.
 Nr5a2. Everest, EB12283. 0.5 µg/mL (IHC, WB). 2 µg/ChIP
 Nr5a2. RD Biosystems, PP-H2325-00. 1 µg/mL (WB). 5 µg/ChIP
 Nr5a2. Sigma, HPA005455. 0.8 µg/mL (IHC), 2µg/mL (IF).
 Phospho c-Jun. Cell Signalling CST, D47G9. 0.6-1 µg/mL (IHC).
 phospho c-Jun. Cell Signalling, 9164. 0.1 µg/mL (IHC).
 Phospho Jnk. Cell Signalling, CST 9251. 0.1 µg/mL (WB).
 Phospho-Erk. CST, #9101. 0.1 µg/mL (WB).
 Phospho-Stat3-Y705. 2 µg/mL (IHC).
 Ptf1a. Kindly provided by B. Bréant, INSERM, Paris. 1/100 (IF).
 Vinculin. Sigma, Clone hVIN-1. 0.1-0.13 µg/mL (WB).

10. Eukaryotic cell lines

a. State the source of each eukaryotic cell line used.

HEK293 cells (ATCC) and 266-6 (I. Rooman, who obtained them from ATCC). Stated in the text.

b. Describe the method of cell line authentication used.

HEK293 cells were not authenticated as they came from ATCC. 266-6 cells are known to the investigators and unique and experimental analyses showed that they are the expected cells (only one mouse cell line with acinar features is available to our knowledge worldwide).

c. Report whether the cell lines were tested for mycoplasma contamination.

Yes, tested and only Mycoplasma-negative cultures were used.

d. If any of the cell lines used are listed in the database of commonly misidentified cell lines maintained by ICLAC, provide a scientific rationale for their use.

No commonly misidentified cell lines were used.

► Animals and human research participants

Policy information about [studies involving animals](#); when reporting animal research, follow the [ARRIVE guidelines](#)

11. Description of research animals

Provide details on animals and/or animal-derived materials used in the study.

Information provided in detail in the Methods section. The following strains of *Mus musculus* were used (and validated): Nr5a2^{+/-}, conditional floxed c-Jun, conditional floxed Nr5a2, LysCre, Ptf1aCre^{+/+} knock-in.

Source of mice and references:

Nr5a2^{+/-} - Botrugno, O. A., et al. Synergy between LRH-1 and beta-catenin induces G1 cyclin-mediated cell proliferation. *Mol. Cell* 15, 499-509 (2004)

Conditional floxed c-Jun - Behrens, A., et al. Impaired postnatal hepatocyte proliferation and liver regeneration in mice lacking c-jun in the liver. *EMBO J.* 21, 1782-1790 (2002).

Conditional floxed Nr5a2 - Coste, A. et al. LRH-1-mediated glucocorticoid synthesis in enterocytes protects against inflammatory bowel disease. *Proc. Natl Acad. Sci. USA* 104, 13098–13103 (2007).

Lys-Cre - Clausen, B. E. et al. Conditional gene targeting in macrophages and granulocytes using LysMcre mice. *Transgenic Res.* 8, 265–277 (1999).

Ptf1a-Cre - Kawaguchi, Y., et al. The role of the transcriptional regulator Ptf1a in converting intestinal to pancreatic progenitors. *Nat. Genet.* 32, 128-134 (2002).

Policy information about [studies involving human research participants](#)

12. Description of human research participants

Describe the covariate-relevant population characteristics of the human research participants.

Information provided in detail in the Methods section. GWAS analyses as described in text.

Source of human pancreata for RNA-Seq as described in text: "Histologically normal fresh frozen pancreatic tissue samples (n=95) either from patients with pancreatic cancer (n=79) (Mayo Clinic, Rochester, MN; Memorial Sloan Kettering Cancer Center, New York, NY) or from organ donors (n=16) (Penn State College of Medicine, Hershey, PA and Gift of Life Donor Program, Philadelphia, PA) were used. Histological review was performed at each participating institution. The project was approved by the Institutional Review Boards of each participating institution as well as the NIH, Bethesda. Subjects of self-reported non-European ancestry and those with history of neo-adjuvant therapy prior to surgery were excluded from the study."

Pancreatic cancer cases, source, and information, as described in Supplementary Table 1.